Journal of King Saud University – Engineering Sciences (2014) **26**, 49–68

King Saud University
Journal of King Saud University – Engineering Sciences
www.ksu.edu.sa
www.sciencedirect.com

ORIGINAL ARTICLE

Mixed convective flow of immiscible fluids in a vertical corrugated channel with traveling thermal waves

J.C. Umavathi *, M. Shekar

Department of Mathematics, Gulbarga University, Gulbarga, Karnataka 585 106, India

Received 29 August 2012; accepted 26 November 2012
Available online 5 December 2012

KEYWORDS
Mixed convection;
Immiscible fluids;
Corrugated channel;
Traveling thermal waves;
Perturbation method

Abstract Fully developed laminar mixed convection in a corrugated vertical channel filled with two immiscible viscous fluids has been investigated. By using a perturbation technique, the coupled nonlinear equations governing the flow and heat transfer are solved. The fluids are assumed to have different viscosities and thermal conductivities. Separate solutions are matched at the interface using suitable matching conditions. The velocity, the temperature, the Nusselt number and the shear stress are analyzed for variations of the governing parameters such as Grashof number, viscosity ratio, width ratio, conductivity ratio, frequency parameter, traveling thermal temperature and are shown graphically. It is found that the Grashof number, viscosity ratio, width ratio and conductivity ratio enhance the velocity parallel to the flow direction and reduce the velocity perpendicular to the flow direction.

1. Introduction

Mixed convection is defined as a heat transfer situation where both natural convection and forced convection heat transfer mechanisms interact. In the past thirty years, mixed convection in a vertical heated channel has received considerable attention due to its extensive practical applications, including turbine rotor blade internal cooling systems, cooling of nuclear reactors and electronic components. From a technological point of view, the study of viscous fluids bounded by corrugated surfaces is of special interest and has practical applications in the cooling of electronic devices and systems, enhancing the heat transfer efficiency of industrial transport processes. The problem of viscous flow in a wavy channel was first treated analytically by Burns and Parks (1967). Later on Goldstein and Sparrow (1977), O'Brien and Sparrow (1982), Vajravelu (1989) and Saniei and Dini (1993) studied the flow through a corrugated channel.

Wang and Vanka (1995) determined the rates of heat transfer for flow through a periodic array of wavy passages. Malashetty et al. (2001a) studied the magnetoconvective flow and heat transfer between a vertical wavy wall and a parallel flat wall. Wang and Chen (2001) analyzed the rate of heat transfer for flow through a sinusoidal curved channel. A numerical study of mixed convection heat and mass transfer along a vertical wavy surface has been carried out by Jang and Yan (2004). Yao (2006) used finite difference methods to analyze the problem of natural convection boundary layer flow along a complex vertical surface represented by two sinusoidal functions. He found that the total heat-transfer rates for a complex surface are greater than those for a flat surface. Kuhn

* Corresponding author. Tel.: +91 9916223260.
E-mail address: jc_uma11@yahoo.com (J.C. Umavathi).
Peer review under responsibility of the King Saud University.

ELSEVIER Production and hosting by Elsevier

1018-3639 © 2012 Production and hosting by Elsevier B.V. on behalf of King Saud University.
http://dx.doi.org/10.1016/j.jksues.2012.11.002

Nomenclature

a	amplitude
$C_p^{(j)}$	specific heat at constant pressure
C_p	ratio of specific heat at constant pressure
g	acceleration due to gravity
Gr	Grashof number $(h^{(1)^3} g\beta^{(1)}\Delta T/v^{(1)^2})$
h	width ratio $(h^{(2)}/h^{(1)})$
$K^{(j)}$	thermal conductivity
k	thermal conductivity ratio $(K^{(2)}/K^{(1)})$
m	viscosity ratio $(\mu^{(1)}/\mu^{(2)})$
Nu	Nusselt number
$P^{(j)}$	pressure
p_s	static pressure
$p^{(j)}$	dimensionless pressure
Pr	Prandtl number $\left(C_p^{(1)}\mu^{(1)}/K^{(1)}\right)$
r	density ratio $(\rho^{(2)}/\rho^{(1)})$
$T^{(j)}$	temperature
$T^{*(j)}, \phi^{(j)}$	dimensionless temperature
T_s	static temperature
t	time
$U^{(j)}, V^{(j)}$	velocities along X and Y directions
$u^{(j)}, v^{(j)}$	dimensionless velocities
$X^{(j)}, Y^{(j)}$	space co-ordinates
$x^{(j)}, y^{(j)}$	dimensionless space co-ordinates

Greek symbols

$\beta^{(j)}$	coefficient of thermal expansion
β	ratio of coefficient of thermal expansion $(\beta^{(2)}/\beta^{(1)})$
ε	dimensionless amplitude parameter $(a/h^{(1)})$
λ	wave length
$\lambda^{(j)}$	dimensionless wave number $(\lambda^{(j)}/h^{(j)})$
$\mu^{(j)}$	viscosity
$v^{(j)}$	kinematic viscosity $(\mu^{(j)}/\rho^{(j)})$
θ	traveling thermal temperature
$\rho^{(j)}$	density
ρ_0	static density
τ	skin friction
ω	frequency parameter
ψ	stream function

Superscript

$j = 1,2$	where 1 and 2 refer quantities for the fluids in region-I and region-II respectively.

Subscript

0	mean part
1	perturbed part

and Rohr (2008) experimentally investigated mixed convective flow over a wavy wall.

One geometry of the flow passage that is very simple and may be used to enhance the exchanger performance is that formed by wavy walls. Wavy channels are easy to fabricate and can provide significant heat transfer enhancement if operated in an appropriate (transitional) Reynolds-number range. Therefore, wavy passages have been considered in several earlier studies as a means to enhance heat/mass transfer in compact exchange devices. Both corrugated and converging-diverging cross-sections have been studied experimentally and numerically. An important observation made is that wavy passages do not provide any significant heat transfer enhancement when the flow is steady. However, if the flow is made unsteady (either through external forcing or through natural transitioning to an unsteady state) significant increases in heat exchange are observed.

In realistic situations, however, the fluid system often consists of two (and possibly more) separate, immiscible liquids, a layer of one liquid overlying a layer of another liquid. The problem formulation now contains additional dynamical ingredients such as the interfacial stresses and the deformation of the interface shape. Also, a multi-layered liquid arrangement provides an improved model for the buoyancy-driven convection process in growing high-quality crystals.

The application of the two-fluid model is dependent on the presumed interface shape (either plane or curved) and on the availability of reliable closure relations for the wall shear and interfacial shear stresses (averaged over the corresponding wetted perimeter) in terms of the local/instantaneous holdup and velocities. These closure relations should correctly represent the effects of the system's parameters (e.g. fluids' flow rates and physical properties).

Meyer and Garder (1954) were the first authors to publish a paper on the mechanics of two immiscible fluids in porous media. Loharsabi and Sahai (1998) analyzed the flow of two immiscible fluids in a parallel plate channel assuming the continuity of velocity and thermal equilibrium at the interface. Several researchers have assumed that separated two-phase flow can be well represented by the superimposition of two single-phase flows separated by a flat interface. The first exact solution for the fluid flow in the interface region was presented in Vafai and Kim (1990). In that study, the shear stress in the fluid and the porous medium were taken to be equal at the interface region. Using this assumption, Malashetty and Leela (1992), Malashetty et al. (2001b, 2004), Umavathi et al. (2005, 2007, 2008a,b) and Prathap Kumar et al. (2011a,b) studied the flow and heat transfer of different immiscible fluids through channels. Most recently Umavathi and Shekar (2011, 2012) studied the mixed convection flow of immiscible fluids in a vertical corrugated channel.

In the literature, numerous experimental and theoretical studies have been reported concerning the heat transfer in the corrugated surface for the one-fluid model. Keeping in view the various applications of the two-fluid model, we were motivated to analyze the flow nature of two immiscible fluids in a vertical corrugated channel for unsteady flow. The temperature and velocity distributions are simulated by the perturbation method.

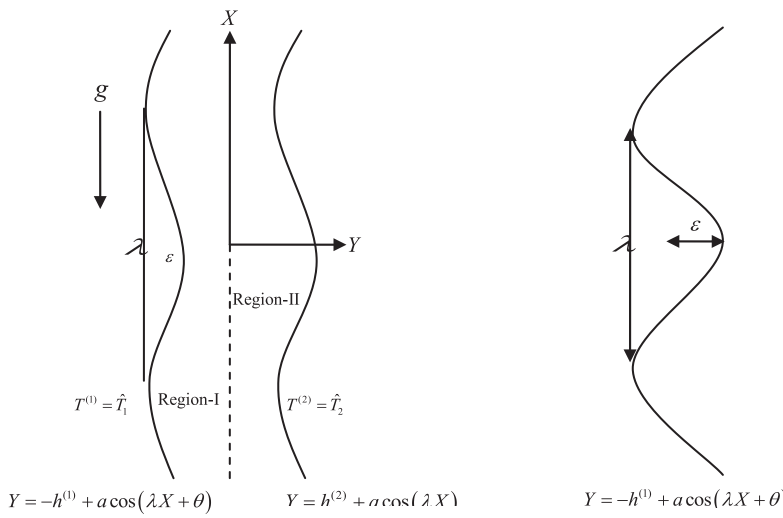

Figure 1 Physical model and the coordinate system.

2. Mathematical formulation of the problem

We consider a two dimensional unsteady laminar mixed convective flow of two immiscible, incompressible fluids in a vertical wavy channel as shown in Fig. 1. The X-axis is taken parallel to the wavy wall, while the Y-axis is taken perpendicular to it in such a way that the left wavy wall is represented by $Y = -h^{(1)} + a\cos(\lambda X + \theta)$ and the right wavy wall by $Y = h^{(2)} + a\cos(\lambda X)$. The values of $\theta = 0,\pi/2,\pi$ and $3\pi/2$ represent different configurations of the wavy channels such as:

(i) the crest of a wall corresponds to the crest of the other wall of the channel;
(ii) one of the walls considered in (i) has a phase-advance/lag;
(iii) the crest of the wall corresponds to the trough of the other; and
(iv) one of the walls considered in (iii) has a phase-advance/lag.

The left and right walls are maintained at constant temperature $\widehat{T}_1$ and $\widehat{T}_2$ respectively. The region $-h^{(1)} + a\cos(\lambda X + \theta) \leqslant Y \leqslant 0$ (region-I) is occupied by a fluid of density $\rho^{(1)}$, viscosity $\mu^{(1)}$, thermal conductivity $K^{(1)}$, thermal expansion coefficient $\beta^{(1)}$, specific heat at a constant temperature $C_p^{(1)}$ and the region $0 \leqslant Y \leqslant h^{(2)} + a\cos(\lambda X)$ (region-II) is occupied by the fluid of density $\rho^{(2)}$, viscosity $\mu^{(2)}$, thermal conductivity $K^{(2)}$, thermal expansion coefficient $\beta^{(2)}$, specific heat at a constant temperature $C_p^{(2)}$. The fluids properties are assumed to be constant except the density in the buoyancy term in the momentum equation. The fluid rises in the channel driven by buoyancy forces. The transport properties of both the fluids are assumed to be constant. The wave length of the wavy wall which is proportional to $1/\lambda$ is very large, where λ is the wave length. Since our model is general, one can choose any two different fluids which are immiscible.

We consider the fluid to be incompressible and the flow is unsteady, laminar, and two-dimensional (that is, the flow is identical in vertical layers, which is a valid assumption). It is assumed that the only non-zero component of the velocity is the X-component $U^{(j)} (j = 1,2)$. Thus, with these assumptions, the continuity equations, the momentum equations, and the energy equations are in the form

Region-I

$$\frac{\partial U^{(1)}}{\partial X^{(1)}} + \frac{\partial V^{(1)}}{\partial Y^{(1)}} = 0 \tag{1}$$

$$\rho^{(1)}\left(\frac{\partial U^{(1)}}{\partial t^{(1)}} + U^{(1)}\frac{\partial U^{(1)}}{\partial X^{(1)}} + V^{(1)}\frac{\partial U^{(1)}}{\partial Y^{(1)}}\right) = -\frac{\partial P^{(1)}}{\partial X^{(1)}} + \mu^{(1)}\left(\frac{\partial^2 U^{(1)}}{\partial X^{(1)2}} + \frac{\partial^2 U^{(1)}}{\partial Y^{(1)2}}\right) - \rho^{(1)}g \tag{2}$$

$$\rho^{(1)}\left(\frac{\partial V^{(1)}}{\partial t^{(1)}} + U^{(1)}\frac{\partial V^{(1)}}{\partial X^{(1)}} + V^{(1)}\frac{\partial V^{(1)}}{\partial Y^{(1)}}\right) = -\frac{\partial P^{(1)}}{\partial Y^{(1)}} + \mu^{(1)}\left(\frac{\partial^2 V^{(1)}}{\partial X^{(1)2}} + \frac{\partial^2 V^{(1)}}{\partial Y^{(1)2}}\right) \tag{3}$$

$$\rho^{(1)}C_p^{(1)}\left(\frac{\partial T^{(1)}}{\partial t^{(1)}} + U^{(1)}\frac{\partial T^{(1)}}{\partial X^{(1)}} + V^{(1)}\frac{\partial T^{(1)}}{\partial Y^{(1)}}\right) = K^{(1)}\left(\frac{\partial^2 T^{(1)}}{\partial X^{(1)2}} + \frac{\partial^2 T^{(1)}}{\partial Y^{(1)2}}\right) \tag{4}$$

$$\rho^{(1)} = \rho_0(1 - \beta^{(1)}(T^{(1)} - T_s)) \tag{5}$$

Region-II

$$\frac{\partial U^{(2)}}{\partial X^{(2)}} + \frac{\partial V^{(2)}}{\partial Y^{(2)}} = 0 \tag{6}$$

$$\rho^{(2)}\left(\frac{\partial U^{(2)}}{\partial t^{(2)}} + U^{(2)}\frac{\partial U^{(2)}}{\partial X^{(2)}} + V^{(2)}\frac{\partial U^{(2)}}{\partial Y^{(2)}}\right) = -\frac{\partial P^{(2)}}{\partial X^{(2)}} + \mu^{(2)}\left(\frac{\partial^2 U^{(2)}}{\partial X^{(2)2}} + \frac{\partial^2 U^{(2)}}{\partial Y^{(2)2}}\right) - \rho^{(2)}g \tag{7}$$

$$\rho^{(2)}\left(\frac{\partial V^{(2)}}{\partial t^{(2)}}+U^{(2)}\frac{\partial V^{(2)}}{\partial X^{(2)}}+V^{(2)}\frac{\partial V^{(2)}}{\partial Y^{(2)}}\right) = -\frac{\partial P^{(2)}}{\partial Y^{(2)}}+\mu^{(2)}\left(\frac{\partial^2 V^{(2)}}{\partial X^{(2)2}}+\frac{\partial^2 V^{(2)}}{\partial Y^{(2)2}}\right) \tag{8}$$

$$\rho^{(2)}C_p^{(2)}\left(\frac{\partial T^{(2)}}{\partial t^{(2)}}+U^{(2)}\frac{\partial T^{(2)}}{\partial X^{(2)}}+V^{(2)}\frac{\partial T^{(2)}}{\partial Y^{(2)}}\right) = K^{(2)}\left(\frac{\partial^2 T^{(2)}}{\partial X^{(2)2}}+\frac{\partial^2 T^{(2)}}{\partial Y^{(2)2}}\right) \tag{9}$$

$$\rho^{(2)} = \rho_0(1-\beta^{(2)}(T^{(2)}-T_s)) \tag{10}$$

A characteristic feature of the two-layer flow problem is the coupling across liquid/liquid interfaces. Interfacial relations can be very complicated for certain practical applications. This is mainly due to the terms arising from mass transfer and from normal stresses. The former contributes as a thrust force due to the density change in the mechanical boundary conditions. The latter introduces complicated coupling effects of the flow fields with the thermodynamic properties at the interface. The liquid layers are mechanically coupled via transfer of momentum across the interfaces. Transfer of momentum results from the continuity of interface tangential velocity and from a stress balance across the interface. Together with these two conditions, continuity of pressure gradient along the flow direction at a liquid–liquid interface is assumed. Thermal coupling is achieved through the continuity of temperature at the interface and the balance of heat transfer across the interface. Along with these there is a "no-slip" condition and a constant temperature at the boundaries. With these assumptions the boundary and interface conditions become

$$\begin{aligned}
&U^{(1)} = V^{(1)} = 0 \quad \text{at } Y = -h^{(1)} + a\cos(\lambda X+\theta)\\
&U^{(2)} = V^{(2)} = 0 \quad \text{at } Y = h^{(2)} + a\cos(\lambda X)\\
&U^{(1)} = U^{(2)}, \qquad V^{(1)} = V^{(2)} \text{ at } Y=0\\
&\mu^{(1)}\left(\frac{\partial U^{(1)}}{\partial Y^{(1)}}+\frac{\partial V^{(1)}}{\partial X^{(1)}}\right) = \mu^{(2)}\left(\frac{\partial U^{(2)}}{\partial Y^{(2)}}+\frac{\partial V^{(2)}}{\partial X^{(2)}}\right) \text{ at } Y=0\\
&\frac{\partial P^{(1)}}{\partial X^{(1)}} = \frac{\partial P^{(2)}}{\partial X^{(2)}} \text{ at } Y=0
\end{aligned} \tag{11}$$

$$\begin{aligned}
&T^{(1)} = T_1(1+a\cos(\lambda X+\omega t))\\
&\quad = \widehat{T}_1 \text{ (say) at } Y = -h^{(1)} + a\cos(\lambda X+\theta)\\
&T^{(2)} = T_2(1+a\cos(\lambda X+\omega t))\\
&\quad = \widehat{T}_2 \text{ (say) at } Y = h^{(2)} + a\cos(\lambda X)\\
&T^{(1)} = T^{(2)}, \quad K^{(1)}\left(\frac{\partial T^{(1)}}{\partial Y^{(1)}}+\frac{\partial T^{(1)}}{\partial X^{(1)}}\right) = K^{(2)}\left(\frac{\partial T^{(2)}}{\partial Y^{(2)}}+\frac{\partial T^{(2)}}{\partial X^{(2)}}\right) \text{ at}\\
&Y=0
\end{aligned} \tag{12}$$

The boundary conditions on the temperature field physically indicate that there are traveling thermal waves moving in a negative X-direction.

We next introduce the non-dimensional flow variables as

$$\begin{aligned}
&x^{(1)} = \frac{X^{(1)}}{h^{(1)}}, \quad y^{(1)} = \frac{Y^{(1)}}{h^{(1)}}, \quad x^{(2)} = \frac{X^{(2)}}{h^{(2)}}, \quad y^{(2)} = \frac{Y^{(2)}}{h^{(2)}},\\
&u^{(1)} = \frac{h^{(1)}}{v^{(1)}}U^{(1)}, \quad v^{(1)} = \frac{h^{(1)}}{v^{(1)}}V^{(1)},\\
&u^{(2)} = \frac{h^{(2)}}{v^{(2)}}U^{(2)}, \quad v^{(2)} = \frac{h^{(2)}}{v^{(2)}}V^{(2)}, \quad p^{(1)} = \frac{P^{(1)}}{\rho^{(1)}(v^{(1)}/h^{(1)})^2},\\
&p^{(2)} = \frac{P^{(2)}}{\rho^{(2)}(v^{(2)}/h^{(2)})^2},\\
&T^{*(1)} = \frac{T^{(1)}-\widehat{T}_1}{\widehat{T}_2-\widehat{T}_1}, \quad T^{*(2)} = \frac{T^{(2)}-\widehat{T}_1}{\widehat{T}_2-\widehat{T}_1}, \quad \beta = \frac{\beta^{(2)}}{\beta^{(1)}}, \quad h = \frac{h^{(2)}}{h^{(1)}},\\
&m = \frac{\mu^{(1)}}{\mu^{(2)}}, \quad r = \frac{\rho^{(2)}}{\rho^{(1)}}, \quad t^{*(1)} = \left(\frac{tv}{h^2}\right)^{(1)},\\
&t^{*(2)} = \left(\frac{tv}{h^2}\right)^{(2)}, \quad k = \frac{K^{(2)}}{K^{(1)}}, \quad Gr = \frac{h^{(1)^3}g\beta^{(1)}\Delta T}{v^{(1)2}},\\
&\Pr = \frac{C_p^{(1)}\mu^{(1)}}{K^{(1)}}, \quad \varepsilon = \frac{a}{h^{(1)}}, \quad \lambda^* = \frac{\lambda}{h^{(1)}}, \quad \Delta T = \widehat{T}_2 - \widehat{T}_1
\end{aligned} \tag{13}$$

In terms of these non-dimensional variables, the basic Eqs. (1)–(4), (6)–(9) can be expressed in the dimensionless form as, (for simplicity, the notation is considered as $x^{(1)} = x$; $y^{(1)} = y$; $t^{*(1)} = t^*$ in region-I and $x^{(2)} = x$; $y^{(2)} = y$; $t^{*(2)} = t^*$ in region-II).

Region-I

$$\frac{\partial u^{(1)}}{\partial x}+\frac{\partial v^{(1)}}{\partial y} = 0 \tag{14}$$

$$\frac{\partial u^{(1)}}{\partial t^*}+u^{(1)}\frac{\partial u^{(1)}}{\partial x}+v^{(1)}\frac{\partial u^{(1)}}{\partial y} = -\frac{\partial p^{(1)}}{\partial x}+\frac{\partial^2 u^{(1)}}{\partial x^2}+\frac{\partial^2 u^{(1)}}{\partial y^2} + GrT^{*(1)} \tag{15}$$

$$\frac{\partial v^{(1)}}{\partial t^*}+u^{(1)}\frac{\partial v^{(1)}}{\partial x}+v^{(1)}\frac{\partial v^{(1)}}{\partial y} = -\frac{\partial p^{(1)}}{\partial y}+\frac{\partial^2 v^{(1)}}{\partial x^2}+\frac{\partial^2 v^{(1)}}{\partial y^2} \tag{16}$$

$$\frac{\partial T^{*(1)}}{\partial t^*}+u^{(1)}\frac{\partial T^{*(1)}}{\partial x}+v^{(1)}\frac{\partial T^{*(1)}}{\partial y} = \frac{1}{\Pr}\left(\frac{\partial^2 T^{*(1)}}{\partial x^2}+\frac{\partial^2 T^{*(1)}}{\partial y^2}\right) \tag{17}$$

Region-II

$$\frac{\partial u^{(2)}}{\partial x}+\frac{\partial v^{(2)}}{\partial y} = 0 \tag{18}$$

$$\frac{\partial u^{(2)}}{\partial t^*}+u^{(2)}\frac{\partial u^{(2)}}{\partial x}+v^{(2)}\frac{\partial u^{(2)}}{\partial y} = -\frac{\partial p^{(2)}}{\partial x}+\frac{\partial^2 u^{(2)}}{\partial x^2}+\frac{\partial^2 u^{(2)}}{\partial y^2} + Gr\beta h^3 m^2 r^2 T^{*(2)} \tag{19}$$

$$\frac{\partial v^{(2)}}{\partial t^*}+u^{(2)}\frac{\partial v^{(2)}}{\partial x}+v^{(2)}\frac{\partial v^{(2)}}{\partial y} = -\frac{\partial p^{(2)}}{\partial y}+\frac{\partial^2 v^{(2)}}{\partial x^2}+\frac{\partial^2 v^{(2)}}{\partial y^2} \tag{20}$$

$$\frac{\partial T^{*(2)}}{\partial t^*}+u^{(2)}\frac{\partial T^{*(2)}}{\partial x}+v^{(2)}\frac{\partial T^{*(2)}}{\partial y} = \frac{kmC_p}{\Pr}\left(\frac{\partial^2 T^{*(2)}}{\partial x^2}+\frac{\partial^2 T^{*(2)}}{\partial y^2}\right) \tag{21}$$

Using (13), the boundary and interface conditions (11) and (12) for the velocity and temperature fields become

$$u^{(1)} = v^{(1)} = 0 \quad \text{at } y = -1 + \varepsilon\cos(\lambda^* x + \theta),$$
$$u^{(2)} = v^{(2)} = 0 \text{ at } y = 1 + \frac{\varepsilon\cos(\lambda^* x)}{h}$$
$$u^{(1)} = \frac{u^{(2)}}{mhr}, \quad v^{(1)} = \frac{v^{(2)}}{mhr} \text{ at } Y = 0,$$
$$\frac{\partial u^{(1)}}{\partial y} + \frac{\partial v^{(1)}}{\partial x} = \frac{1}{m^2h^2r}\left(\frac{\partial u^{(2)}}{\partial y} + \frac{\partial v^{(2)}}{\partial x}\right) \quad \text{at } y = 0$$
$$\frac{\partial p^{(1)}}{\partial x} = \frac{1}{rm^2h^3}\frac{\partial p^{(2)}}{\partial x} \quad \text{at } y = 0 \tag{22}$$
$$T^{*(1)} = 0 \text{ at } y = -1 + \varepsilon\cos(\lambda^* x + \theta), T^{*(2)} = 1$$
$$\text{at } y = 1 + \frac{\varepsilon\cos(\lambda^* x)}{h}$$
$$T^{*(1)} = T^{*(2)}, \quad \frac{\partial T^{*(1)}}{\partial y} + \frac{\partial T^{*(1)}}{\partial x} = \frac{k}{h}\left(\frac{\partial T^{*(2)}}{\partial y} + \frac{\partial T^{*(2)}}{\partial x}\right)$$
$$\text{at } y = 0 \tag{23}$$

In the static fluid we have (see Vajravelu and Sastri, 1978)

$$0 = -\frac{\partial p_s}{\partial x} - \frac{\rho_s g h^{(1)3}}{\rho v^{(1)2}} = -\frac{\partial p_s}{\partial x} - \frac{\rho_s g h^{(2)3}}{\rho v^{(2)2}} \tag{24}$$

In view of (24). Eqs. (15) and (19) becomes

$$\frac{\partial u^{(1)}}{\partial t^*} + u^{(1)}\frac{\partial u^{(1)}}{\partial x} + v^{(1)}\frac{\partial u^{(1)}}{\partial y} = -\frac{\partial (p^{(1)} - p_s)}{\partial x} + \frac{\partial^2 u^{(1)}}{\partial x^2} + \frac{\partial^2 u^{(1)}}{\partial y^2} + GrT^{*(1)} \tag{25}$$

$$\frac{\partial u^{(2)}}{\partial t^*} + u^{(2)}\frac{\partial u^{(2)}}{\partial x} + v^{(2)}\frac{\partial u^{(2)}}{\partial y} = -\frac{\partial (p^{(2)} - p_s)}{\partial x} + \frac{\partial^2 u^{(2)}}{\partial x^2} + \frac{\partial^2 u^{(2)}}{\partial y^2} + Gr\beta h^3 m^2 r^2 T^{*(2)} \tag{26}$$

3. Solutions

Eq. (14), (16)–(18), (20), (21), (25), and (26) are coupled non-linear and are to be solved simultaneously. Due to the non-linearity, analytical solutions are difficult; however approximate solutions can be obtained using perturbation techniques. Assuming that the solutions consist of a mean part and a perturbed part, velocity, pressure and temperature can be written as,

$$u(x, y, t^*) = u_0(y) + u_1(x, y, t^*) \tag{27}$$
$$v(x, y, t^*) = v_1(x, y, t^*) \tag{28}$$
$$p(x, y, t^*) = p_0(x, y, t^*) + p_1(x, y, t^*) \tag{29}$$
$$T^*(x, y, t^*) = T_0^*(y) + T_1^*(x, y, t^*) \tag{30}$$

where the perturbed quantities u_1,v_1,p_1 and T_1^* are small compared with the mean or zeroth order quantities. The asterisk on T,t and λ is removed for the sake of simplicity in the following process.

Using (27)–(30) in (14), (16)–(18), (20), (21), (25), and (26) and separating mean and perturbed parts, gives the following equations.

Zeroth order equations

Region-I

$$\frac{d^2T_0^{(1)}}{dy^2} = 0 \tag{31}$$
$$\frac{d^2u_0^{(1)}}{dy^2} + GrT_0^{(1)} = 0 \tag{32}$$

Region-II

$$\frac{d^2T_0^{(2)}}{dy^2} = 0 \tag{33}$$
$$\frac{d^2u_0^{(2)}}{dy^2} + Gr\beta h^3 m^2 r^2 T_0^{(2)} = 0 \tag{34}$$

where $\frac{\partial}{\partial x}\left(p_0^{(j)} - p_s\right)$ is taken to be zero (see Ostrach, 1952) for $j = 1,2$.

First order equations

Region-I

$$\frac{\partial u_1^{(1)}}{\partial x} + \frac{\partial v_1^{(1)}}{\partial y} = 0 \tag{35}$$

$$\frac{\partial u_1^{(1)}}{\partial t} + u_0^{(1)}\frac{\partial u_1^{(1)}}{\partial x} + v_1^{(1)}\frac{du_0^{(1)}}{dy} = -\frac{\partial p_1^{(1)}}{\partial x} + \frac{\partial^2 u_1^{(1)}}{\partial x^2} + \frac{\partial^2 u_1^{(1)}}{\partial y^2} + GrT_1^{(1)} \tag{36}$$

$$\frac{\partial v_1^{(1)}}{\partial t} + u_0^{(1)}\frac{\partial v_1^{(1)}}{\partial x} = -\frac{\partial p_1^{(1)}}{\partial y} + \frac{\partial^2 v_1^{(1)}}{\partial x^2} + \frac{\partial^2 v_1^{(1)}}{\partial y^2} \tag{37}$$

$$\frac{\partial T_1^{(1)}}{\partial t} + u_0^{(1)}\frac{\partial T_1^{(1)}}{\partial x} + v_1^{(1)}\frac{dT_0^{(1)}}{dy} = \frac{1}{\mathrm{Pr}}\left(\frac{\partial^2 T_1^{(1)}}{\partial x^2} + \frac{\partial^2 T_1^{(1)}}{\partial y^2}\right) \tag{38}$$

Region-II

$$\frac{\partial u_1^{(2)}}{\partial x} + \frac{\partial v_1^{(2)}}{\partial y} = 0 \tag{39}$$

$$\frac{\partial u_1^{(2)}}{\partial t} + u_0^{(2)}\frac{\partial u_1^{(2)}}{\partial x} + v_1^{(2)}\frac{du_0^{(2)}}{dy} = -\frac{\partial p_1^{(2)}}{\partial x} + \frac{\partial^2 u_1^{(2)}}{\partial x^2} + \frac{\partial^2 u_1^{(2)}}{\partial y^2} + Gr\beta h^3 m^2 r^2 T_1^{(2)} \tag{40}$$

$$\frac{\partial v_1^{(2)}}{\partial t} + u_0^{(2)}\frac{\partial v_1^{(2)}}{\partial x} = -\frac{\partial p_1^{(2)}}{\partial y} + \frac{\partial^2 v_1^{(2)}}{\partial x^2} + \frac{\partial^2 v_1^{(2)}}{\partial y^2} \tag{41}$$

$$\frac{\partial T_1^{(2)}}{\partial t} + u_0^{(2)}\frac{\partial T_1^{(2)}}{\partial x} + v_1^{(1)}\frac{dT_0^{(2)}}{dy} = \frac{kmC_p}{\mathrm{Pr}}\left(\frac{\partial^2 T_1^{(2)}}{\partial x^2} + \frac{\partial^2 T_1^{(2)}}{\partial y^2}\right) \tag{42}$$

In view of (27)–(30) the boundary and interface conditions (22) and (23) can be split as follows,

Zeroth order boundary and interface conditions for velocity and temperature are

$$u_0^{(1)} = 0 \quad \text{at } y = -1, \quad u_0^{(2)} = 0 \quad \text{at } y = 1,$$
$$u_0^{(1)} = \frac{1}{mhr}u_0^{(2)}, \quad \frac{du_0^{(1)}}{dy} = \frac{1}{m^2h^2r}\frac{du_0^{(2)}}{dy} \quad \text{at } y = 0 \tag{43}$$

$$T_0^{(1)} = 0 \quad \text{at } y = -1, \quad T_0^{(2)} = 1 \quad \text{at } y = 1,$$

$$T_0^{(1)} = T_0^{(2)}, \quad \frac{dT_0^{(1)}}{dy} = \frac{k}{h}\frac{dT_0^{(2)}}{dy} \quad \text{at } y = 0 \tag{44}$$

First order boundary and interface conditions for velocity and temperature are

$$u_1^{(1)} = -\cos(\lambda x + \theta)\frac{du_0^{(1)}}{dy}, \quad v_1^{(1)} = 0 \quad \text{at } y = -1,$$

$$u_1^{(2)} = -\frac{\cos(\lambda x)}{h}\frac{du_0^{(2)}}{dy}, \quad v_1^{(2)} = 0 \quad \text{at } y = 1$$

$$u_1^{(1)} = \frac{1}{mhr}u_1^{(2)}, \quad v_1^{(1)} = \frac{1}{mhr}v_1^{(2)} \quad \text{at } y = 0,$$

$$\frac{\partial u_1^{(1)}}{\partial y} + \frac{\partial v_1^{(1)}}{\partial x} = \frac{1}{m^2h^2r}\left(\frac{\partial u_1^{(2)}}{\partial y} + \frac{\partial v_1^{(2)}}{\partial x}\right) \quad \text{at } y = 0$$

$$\frac{\partial p_1^{(1)}}{\partial x} = \frac{1}{rm^2h^3}\frac{\partial p_1^{(2)}}{\partial x} \quad \text{at } y = 0 \tag{45}$$

$$T_1^{(1)} = -\cos(\lambda x + \theta)\frac{dT_0^{(1)}}{dy} \quad \text{at } y = -1,$$

$$T_1^{(2)} = -\frac{\cos(\lambda x)}{h}\frac{dT_0^{(2)}}{dy} \quad \text{at } y = 1$$

$$T_1^{(1)} = T_1^{(2)}, \quad \frac{\partial T_1^{(1)}}{\partial y} + \frac{\partial T_1^{(1)}}{\partial x} = \frac{k}{h}\left(\frac{\partial T_1^{(2)}}{\partial y} + \frac{\partial T_1^{(2)}}{\partial x}\right) \text{ at } y = 0 \tag{46}$$

In order to solve (35)–(42), for the first order quantities it is convenient to introduce stream function $\bar{\psi}$ in the following form

$$u_1^{(j)} = -\frac{\partial \bar{\psi}^{(j)}}{\partial y} \quad \text{and} \quad v_1^{(j)} = \frac{\partial \bar{\psi}^{(j)}}{\partial x} \text{ for } j = 1, 2 \tag{47}$$

The stream function approach reduces the number of dependent variables to be solved and also eliminates pressure from the list of variables. Differentiate (36) with respect to y and differentiate (37) with respect to x and then subtract (36) with (37) which will result in the elimination of pressure $p_1^{(1)}$. Similar procedure is opted for the elimination of pressure $p_1^{(2)}$ from (40) and (41). Eqs. (35)–(42) after the elimination of $p_1^{(1)}$ and $p_1^{(2)}$, can be expressed in terms of the stream function $\bar{\psi}$ in the form

Region-I

$$\bar{\psi}_{xxt}^{(1)} + \bar{\psi}_{tyy}^{(1)} + u_0^{(1)}\bar{\psi}_{xyy}^{(1)} - \bar{\psi}_x^{(1)}u_{0_{yy}}^{(1)} + u_0^{(1)}\bar{\psi}_{xxx}^{(1)} - \bar{\psi}_{xxxx}^{(1)}$$
$$- \bar{\psi}_{yyyy}^{(1)} - 2\bar{\psi}_{xxyy}^{(1)} + GrT_{1_y}^{(1)} = 0 \tag{48}$$

$$T_{1t}^{(1)} + u_0^{(1)}T_{1x}^{(1)} + \bar{\psi}_x^{(1)}T_{0y}^{(1)} = \frac{1}{\Pr}\left(T_{1xx}^{(1)} + T_{1yy}^{(1)}\right) \tag{49}$$

Region-II

$$\bar{\psi}_{xxt}^{(2)} + \bar{\psi}_{yyt}^{(2)} + u_0^{(2)}\bar{\psi}_{xyy}^{(2)} - \bar{\psi}_x^{(2)}u_{0yy}^{(2)} + u_0^{(2)}\bar{\psi}_{xxx}^{(2)} - \bar{\psi}_{yyyy}^{(2)}$$
$$- \bar{\psi}_{xxxx}^{(2)} - 2\bar{\psi}_{xxyy}^{(2)} + Gr\beta h^3m^2r^2T_{1y}^{(2)} = 0 \tag{50}$$

$$T_{1t}^{(2)} + u_0^{(2)}T_{1x}^{(2)} + \bar{\psi}_x^{(2)}T_{0y}^{(2)} = \frac{kmC_p}{\Pr}\left(T_{1xx}^{(2)} + T_{1yy}^{(2)}\right) \tag{51}$$

where a suffix x or y represents derivative with respect to x or y.

The corresponding boundary and interface conditions on velocity and temperature reduces to

$$\bar{\psi}_y^{(1)} = \cos(\lambda x + \theta)u_{0y}^{(1)}, \quad \bar{\psi}_x^{(1)} = 0 \quad \text{at } y = -1,$$

$$\bar{\psi}_y^{(2)} = \frac{\cos(\lambda x)}{h}u_{0y}^{(2)}, \quad \bar{\psi}_x^{(2)} = 0 \quad \text{at } y = 1$$

$$\bar{\psi}_y^{(1)} = \frac{\bar{\psi}_y^{(2)}}{mhr}, \quad \bar{\psi}_x^{(1)} = \frac{\bar{\psi}_x^{(2)}}{mhr}, \quad \bar{\psi}_{xx}^{(1)} - \bar{\psi}_{yy}^{(1)} = \frac{\bar{\psi}_{xx}^{(2)} - \bar{\psi}_{yy}^{(2)}}{m^2h^2r} \quad \text{at}$$
$$y = 0$$

$$\bar{\psi}_{ty}^{(1)} - \bar{\psi}_x^{(1)}u_{0y}^{(1)} + u_0^{(1)}\bar{\psi}_{xy}^{(1)} - \bar{\psi}_{xxy}^{(1)} - \bar{\psi}_{yyy}^{(1)} + GrT_1^{(1)}$$
$$= \frac{1}{rm^2h^3}\left(\bar{\psi}_{ty}^{(2)} - \bar{\psi}_x^{(2)}u_{0y}^{(2)} + u_0^{(2)}\bar{\psi}_{xy}^{(2)} - \bar{\psi}_{xxy}^{(2)} - \bar{\psi}_{yyy}^{(2)}\right.$$
$$\left. + Gr\beta h^3m^2r^2T_1^{(2)}\right) \quad \text{at } y = 0 \tag{52}$$

$$T_1^{(1)} = -\cos(\lambda x + \theta)T_{0y}^{(1)} \quad \text{at } y = -1,$$

$$T_1^{(2)} = -\frac{\cos(\lambda x)}{h}T_{0y}^{(2)} \quad \text{at } y = 1$$

$$T_1^{(1)} = T_1^{(2)}, \quad T_{1xx}^{(1)} + T_{1yy}^{(1)} = \frac{k(T_{1xx}^{(2)} + T_{1yy}^{(2)})}{h} \text{ at } y = 0 \tag{53}$$

We assume stream function and temperature in the following form

$$\bar{\psi}^{(j)} = \varepsilon e^{i(\lambda x + \omega t)}\psi^{(j)}(y), \quad T_1^{(j)} = \varepsilon e^{i(\lambda x + \omega t)}\phi^{(j)}(y) \text{ for } j = 1, 2 \tag{54}$$

from which we infer

$$u_1(x, y, t) = \varepsilon e^{i(\lambda x + \omega t)}u_1(y), \quad v_1(x, y, t) = \varepsilon e^{i(\lambda x + \omega t)}v_1(y) \tag{55}$$

where i is the imaginary unit.

In view of (54), (48)–(51) becomes

Region-I

$$\psi_{yyyy}^{(1)} - \left(i\omega + i\lambda u_0^{(1)} + 2\lambda^2\right)\psi_{yy}^{(1)}$$
$$+ \left(i\omega\lambda^2 + i\lambda u_{0yy}^{(1)} + iu_0^{(1)}\lambda^3 + \lambda^4\right)\psi^{(1)} - Gr\phi_y^{(1)} = 0 \tag{56}$$

$$i(\omega\phi^{(1)} + \lambda u_0^{(1)}\phi^{(1)} + \lambda T_{0y}^{(1)}\psi^{(1)}) = \frac{1}{\Pr}\left(-\lambda^2\phi^{(1)} + \phi_{yy}^{(1)}\right) \tag{57}$$

Region-II

$$\psi_{yyyy}^{(2)} - \left(i\omega + i\lambda u_0^{(2)} + 2\lambda^2\right)\psi_{yy}^{(2)}$$
$$+ \left(i\omega\lambda^2 + i\lambda u_{0yy}^{(2)} + i\lambda^3 + \lambda^4\right)\psi^{(2)} - Gr\beta h^3m^2r^2\phi_y^{(2)} = 0 \tag{58}$$

$$i\left(\omega\phi^{(2)} + \lambda u_0^{(2)}\phi^{(2)} + \lambda T_{0y}^{(2)}\psi^{(2)}\right)$$
$$= \frac{kmC_p}{\Pr}\left(-\lambda^2\phi^{(2)} + \phi_{yy}^{(2)}\right) \tag{59}$$

Boundary and interface conditions (52) and (53) can be written in terms of $\psi^{(j)}$ and $\phi^{(j)}$ as

$$\frac{\partial\psi^{(1)}}{\partial y} = \cos(\omega t - \theta)\frac{du_0^{(1)}}{dy}, \quad \psi^{(1)} = 0 \text{ at } y = -1,$$

$$\frac{\partial\psi^{(2)}}{\partial y} = \frac{\cos(\omega t)}{h}\frac{du_0^{(2)}}{dy}, \psi^{(2)} = 0 \text{ at } y = 1$$

$$\psi_y^{(2)} = \frac{\psi_y^{(1)}}{mhr}, \psi^{(1)} = \frac{\psi^{(2)}}{mhr}, \psi_{yy}^{(1)} + \lambda^2\psi^{(1)} = \frac{\psi_{yy}^{(2)} + \lambda^2\psi^{(2)}}{m^2h^2r} \text{ at } y = 0$$

$$i\lambda\psi^{(1)}u_{0y}^{(1)} - \left(i\lambda u_0^{(1)} + i\omega + \lambda^2\right)\psi_y^{(1)} + \psi_{yyy}^{(1)} - Gr\phi^{(1)} = \frac{1}{rm^2h^3}\left(i\lambda\psi^{(2)}u_{0y}^{(2)} - \left(i\lambda u_0^{(2)} + i\omega\right)\psi_y^{(2)} + \lambda^2\psi_y^{(2)} + \psi_{yyy}^{(2)} - Gr\beta m^2r^2h^3\phi^{(2)}\right) \quad \text{at } y = 0 \tag{60}$$

$$\phi^{(1)} = -\cos(\omega t - \theta)\frac{dT_0^{(1)}}{dy} \text{ at } y = -1,$$

$$\phi^{(2)} = -\frac{\cos(\omega t)}{h}\frac{dT_0^{(2)}}{dy} \text{ at } y = 1$$

$$\phi^{(1)} = \phi^{(2)}, \quad \phi_y^{(1)} + i\lambda\phi^{(1)} = \frac{k}{h}\left(\phi_y^{(2)} + i\lambda\phi^{(2)}\right) \quad \text{at } y = 0 \tag{61}$$

We restrict our attention to the real parts of the solutions for the perturbed quantities ψ,ϕ,u_1 and v_1.

Consider only small values of λ on substituting

$$\psi(\lambda, y) = \sum_{n=0}^{\infty}\lambda^n\psi_n, \quad \phi(\lambda, y) = \sum_{n=0}^{\infty}\lambda^n\phi_n \tag{62}$$

into (56)–(60) we obtain to the order of λ, the following set of ordinary differential equations

Zeroth order equations

$$\frac{d^2\phi_{10}}{dy^2} - i\mathrm{Pr}\omega\phi_{10} = 0$$

$$\frac{d^4\psi_{10}}{dy^4} - i\omega\frac{d^2\psi_{10}}{dy^2} - Gr\frac{d\phi_{10}}{dy} = 0$$

$$\frac{d^2\phi_{20}}{dy^2} - \frac{i\omega\mathrm{Pr}}{kmC_p}\phi_{20} = 0$$

$$\frac{d^4\psi_{20}}{dy^4} - i\omega\frac{d^2\psi_{20}}{dy^2} - Gr\beta h^3m^2r^2\frac{d\phi_{20}}{dy} = 0 \tag{63}$$

First order equations

$$\frac{d^2\phi_{11}}{dy^2} - i\omega\mathrm{Pr}\phi_{11} = i\mathrm{Pr}\left(u_0^{(1)}\phi_{10} + \frac{dT_0^{(1)}}{dy}\psi_{10}\right)$$

$$\frac{d^4\psi_{11}}{dy^4} - i\omega\frac{d^2\psi_{11}}{dy^2} = i\left(u_0^{(1)}\frac{d^2\psi_{10}}{dy^2} - \frac{d^2u_0^{(1)}}{dy^2}\psi_{10}\right) + Gr\frac{d\phi_{11}}{dy}$$

$$\frac{d^2\phi_{21}}{dy^2} - \frac{i\omega\mathrm{Pr}}{kmC_p}\phi_{21} = i\frac{\mathrm{Pr}}{kmC_p}\left(u_0^{(2)}\phi_{20} + \frac{dT_0^{(2)}}{dy}\psi_{20}\right)$$

$$\frac{d^4\psi_{21}}{dy^4} - i\omega\frac{d^2\psi_{21}}{dy^2} = i\left(u_0^{(2)}\frac{d^2\psi_{20}}{dy^2} - \frac{d^2u_0^{(2)}}{dy^2}\psi_{20}\right) + Gr\beta h^3m^2r^2\frac{d\phi_{21}}{dy} \tag{64}$$

Zeroth order boundary and interface conditions in terms of stream function and temperature are

$$\frac{d\psi_{10}}{dy} = \cos(\omega t - \theta)\frac{du_0^{(1)}}{dy}, \quad \psi_{10} = 0 \text{ at } y = -1,$$

$$\frac{d\psi_{20}}{dy} = \frac{\cos(\omega t)}{h}\frac{du_0^{(2)}}{dy}, \psi_{20} = 0 \text{ at } y = 1$$

$$\frac{d\psi_{10}}{dy} = \frac{1}{mhr}\frac{d\psi_{20}}{dy}, \quad \psi_{10} = \frac{1}{mhr}\psi_{20},$$

$$\frac{d^2\psi_{10}}{dy^2} = \frac{1}{m^2h^2r}\frac{d^2\psi_{20}}{dy^2} \quad \text{at } y = 0$$

$$\frac{d^3\psi_{10}}{dy^3} - i\omega\frac{d\psi_{10}}{dy} - Gr\phi_{10} = \frac{1}{rm^2h^3}\left(\frac{d^3\psi_{20}}{dy^3} - i\omega\frac{d\psi_{20}}{dy} - Gr\beta h^3m^2r^2\phi_{20}\right) \quad \text{at } y = 0$$

$$\phi_{10} = -\cos(\omega t - \theta)\frac{dT_0^{(1)}}{dy} \text{ at } y = -1,$$

$$\phi_{20} = -\frac{\cos(\omega t)}{h}\frac{dT_0^{(2)}}{dy} \quad \text{at } y = 1$$

$$\phi_{10} = \phi_{20}, \quad \frac{d\phi_{10}}{dy} = \frac{k}{h}\frac{d\phi_{20}}{dy} \text{ at } y = 0 \tag{65}$$

The first order boundary and interface conditions in terms of stream function and temperature are

$$\frac{d\psi_{11}}{dy} = 0, \quad \psi_{11} = 0 \text{ at } y = -1, \frac{d\psi_{21}}{dy} = 0, \psi_{21} = 0 \quad \text{at } y = 1$$

$$\psi_{11} = \frac{\psi_{21}}{mhr}, \quad \frac{d\psi_{11}}{dy} = \frac{1}{mhr}\frac{d\psi_{21}}{dy}, \quad \frac{d^2\psi_{11}}{dy^2} = \frac{1}{m^2h^2r}\frac{d^2\psi_{21}}{dy^2} \quad \text{at } y = 0$$

$$i\frac{du_0^{(1)}}{dy}\psi_{10} - iu_0^{(1)}\frac{d\psi_{10}}{dy} + \frac{d^3\psi_{11}}{dy^3} - i\omega\frac{d\psi_{11}}{dy} - Gr\phi_{11} = \frac{1}{rm^2h^3}\left(i\frac{du_0^{(2)}}{dy}\psi_{20} - iu_0^{(2)}\frac{d\psi_{20}}{dy} + \frac{d^3\psi_{21}}{dy^3} - i\omega\frac{d\psi_{21}}{dy} - Gr\beta h^3m^2r^2\phi_{21}\right) \quad \text{at } y = 0$$

$$\phi_{11} = 0 \text{ at } y = -1, \phi_{21} = 0 \quad \text{at } y = 1$$

$$\phi_{11} = \phi_{21}, \quad \frac{d\phi_{11}}{dy} + i\phi_{10} = \frac{k}{h}\left(\frac{d\phi_{21}}{dy} + i\phi_{20}\right) \quad \text{at } y = 0 \tag{66}$$

The set of Eqs. (31)–(34) subjected to boundary and interface conditions (43) and (44) have been solved exactly for $u_0^{(j)}$ and $T_0^{(j)}$, and the set of Eqs. (63) and (64) subject to boundary and interface conditions (65) and (66) have been solved exactly for ψ_j and $\phi_j (j = 1, 2)$. The solutions are given in the appendix section. From these solutions, the first order quantities can be put in the form,

$$\psi_j = (\psi_r + i\psi_i)^{(j)} = \psi_{0r}^{(j)} + \lambda\psi_{1i}^{(j)}, \quad \phi_j = (\phi_r + i\phi_i)^{(j)} = \phi_{0r}^{(j)} + \lambda\phi_{1i}^{(j)} \quad (j = 1, 2) \tag{67}$$

Suffix r denotes the real part and i denotes the imaginary part

Considering only the real part, the expression for first order velocity and temperature become

$$u_1^{(j)}(x,y,t) = \varepsilon\left(-\cos(\lambda x+\omega t)\frac{d\psi_{j0}}{dy} + \lambda\sin(\lambda x+\omega t)\frac{d\psi_{j1}}{dy}\right) \quad (68)$$

$$v_1^{(j)}(x,y,t) = \varepsilon\left(-\lambda\psi_{j0}\sin(\lambda x+\omega t) - \lambda^2\psi_{j1}\cos(\lambda x+\omega t)\right) \quad (69)$$

$$T_1^{(j)}(x,y,t) = \varepsilon(\cos(\lambda x+\omega t)\phi_{j0} - \lambda\sin(\lambda x+\omega t)\phi_{j1}) \quad (70)$$

The total solutions for the velocity and temperature become the summation of the mean and perturbed parts.

3.1. Skin friction and Nusselt number

The shearing stress τ_{xy} at any point in the fluid is given in non-dimensional form by

$$\tau_{xy} = \left(\frac{h^{(j)2}}{\rho^{(j)}\upsilon^{(j)2}}\right)\overline{\tau}_{xy} = \frac{\partial u^{(j)}}{\partial y} + \frac{\partial v^{(j)}}{\partial x} \quad (71)$$

At the wavy walls $y=-1+\varepsilon\cos(\lambda x+\theta)$ and $y=1+\frac{\varepsilon\cos(\lambda x)}{h}$, the skin friction τ_{xy} becomes

$$\tau_{-1} = \tau_{-1}^0 + \varepsilon Re\left(e^{i(\lambda x+\theta)}\frac{d^2u_0^{(1)}}{dy^2}(-1) + \frac{du_1^{(1)}}{dy}(-1)\right) \quad (72)$$

and

$$\tau_1 = \tau_1^0 + \varepsilon Re\left(\frac{1}{h}e^{i\lambda x}\frac{d^2u_0^{(2)}}{dy^2}(1) + \frac{du_1^{(2)}}{dy}(1)\right) \quad (73)$$

respectively, where $\tau_{-1}^0 = \left(\frac{du_0^{(1)}}{dy}\right)_{y=-1}$ and $\tau_1^0 = \left(\frac{du_0^{(2)}}{dy}\right)_{y=1}$

The dimensionless Nusselt number is given by

$$d = -\frac{K^{(j)}(\widehat{T}_2-\widehat{T}_1)}{h^{(j)}}\left(\frac{dT_0^{(j)}(y)}{dy} + Re(\varepsilon e^{i(\lambda x+\omega t)}\phi^{(j)}(y))\right)$$

or

$$Nu = -\frac{dh^{(j)}}{K^{(j)}(\widehat{T}_2-\widehat{T}_1)} = \frac{dT_0^{(j)}(y)}{dy} + Re\left(\varepsilon e^{i(\lambda x+\omega t)}\phi^{(j)}(y)\right) \quad (74)$$

At the wavy walls $y=-1+\varepsilon\cos(\lambda x+\theta)$ and $y=1+\frac{\varepsilon\cos(\lambda x)}{h}$, Eq. (74) assumes the form

$$Nu_{-1} = Nu_{-1}^0 + \varepsilon Re\left(e^{i(\lambda x+\theta)}\frac{d^2T_0^{(1)}}{dy^2}(-1) + e^{i(\lambda x+\omega t)}\frac{d\phi^{(1)}}{dy}(-1)\right) \quad (75)$$

and

$$Nu_1 = Nu_1^0 + \varepsilon Re\left(\frac{e^{i\lambda x}}{h}\frac{d^2T_0^{(2)}}{dy^2}(1) + e^{i(\lambda x+\omega t)}\frac{d\phi^{(2)}}{dy}(1)\right) \quad (76)$$

respectively, where $Nu_{-1}^0 = \left(\frac{dT_0^{(1)}}{dy}\right)_{y=-1}$ and $Nu_1^0 = \left(\frac{dT_0^{(2)}}{dy}\right)_{y=1}$

where Re represents the real part.

Velocity and temperature solutions are numerically evaluated for several sets of values of the parameters such as, Grashof number Gr, viscosity ratio m, width ratio h, conductivity ratio k, frequency parameter ω and traveling thermal temperature θ. Also, the wall skin friction τ_{-1},τ_1 and the wall Nusselt number Nu_{-1},Nu_1 are calculated numerically and some of the qualitative interesting features are presented graphically.

4. Results and discussion

Analytical solution for the unsteady mixed convection of two immiscible viscous fluids in a vertical wavy channel is analyzed. The non-linear equations are solved by a linearization technique wherein the flow is assumed to be in two parts; a mean part and a perturbed part. Exact solutions are obtained for the mean part and the perturbed part is solved using the long wave approximation. The continuity of velocity, pressure gradient along the flow direction, temperature, shear stress and heat flux across the interface are assumed. The solutions of zeroth order velocity u_0 and the zeroth order temperature T_0 are applicable to the case of a channel both of whose walls are flat. The solutions for mean part (u_0, T_0) and perturbed part (u_1, v_1, T_1) are evaluated numerically and represented graphically for various governing parameters in Figs. 2–14. In all the graphs density ratio, the ratio of thermal expansion coefficient, ratio of specific heat at constant pressure, Prandtl number, wave number, amplitude parameter, ωt and λx are fixed as 1, 1, 1, 0.7, 0.02, 0.02, $\pi/4$,$\pi/2$ respectively for all the computations, whereas the Grashof number, viscosity ratio, width ratio, conductivity ratio, frequency parameter and traveling thermal temperature θ are fixed as 5, 1, 1, 1, 10, 0 respectively for all the graphs except the varying the parameters which are shown in Figs. 2–14.

The behavior of the non-dimensional velocity with changes in the Grashof number Gr is shown in Fig. 2. The effect of the Grashof number on zeroth order velocity u_0 is to increase the velocity in both the regions. The effect of the Grashof number on the first order velocity u_1 is to increase the velocity in region-I ($-1 \leqslant y \leqslant 0.2$ approximately) and then decreases in region-II $0.2 \leqslant y \leqslant 1$ as seen in Fig. 2b. The behavior of total fluid velocity u is same as that of zeroth order velocity as seen in Fig. 2c. Physically, an increase in the value of the Grashof number means an increase in the buoyancy force which supports the motion. Fig. 2d depicts the effect of velocity v perpendicular to the channel length on the Grashof number and it is noticed that the velocity v diminishes sharply as the Grashof number increases.

Fig. 3 shows the effect of viscosity ratio $m(=\mu^{(1)}/\mu^{(2)})$ on the velocity. As the viscosity ratio m increases the zeroth order velocity increases in both the regions, whereas its effect is more dominant in the region-II when compared to region-I as seen in Fig. 3a for values of $m \geqslant 1$. Fig. 3b depicts the variations of viscosity ratio m on the first order velocity. As the viscosity ratio m increases, first order velocity u_1 increases from $y=-1$ to $y=0.4$ (approximately) and it decreases from $y=0.4$ to 1 and its effect is more dominant near the right wavy wall. The effect of viscosity ratio on total fluid velocity u shows the similar nature as that for zeroth order velocity as seen in Fig. 3c. Physically, as m increases, the fluid becomes more viscous in region-I and hence velocity is reduced in region-I when compared to region-II. Hence the velocity is more operative in region-II for variations of viscosity ratio. Fig. 3d shows the behavior of the fluid velocity v perpendicular to the channel length. It is noticed that as the viscosity ratio increases, v decreases in both the regions and the effect of viscosity ratio are more effective in region-II compared to region-I.

The viscosity ratio $m(=\mu^{(1)}/\mu^{(2)})$ does not affect the zeroth order temperature profiles as seen in Fig. 4a. From Fig. 4b it is seen that the first order temperature T_1 increases as the

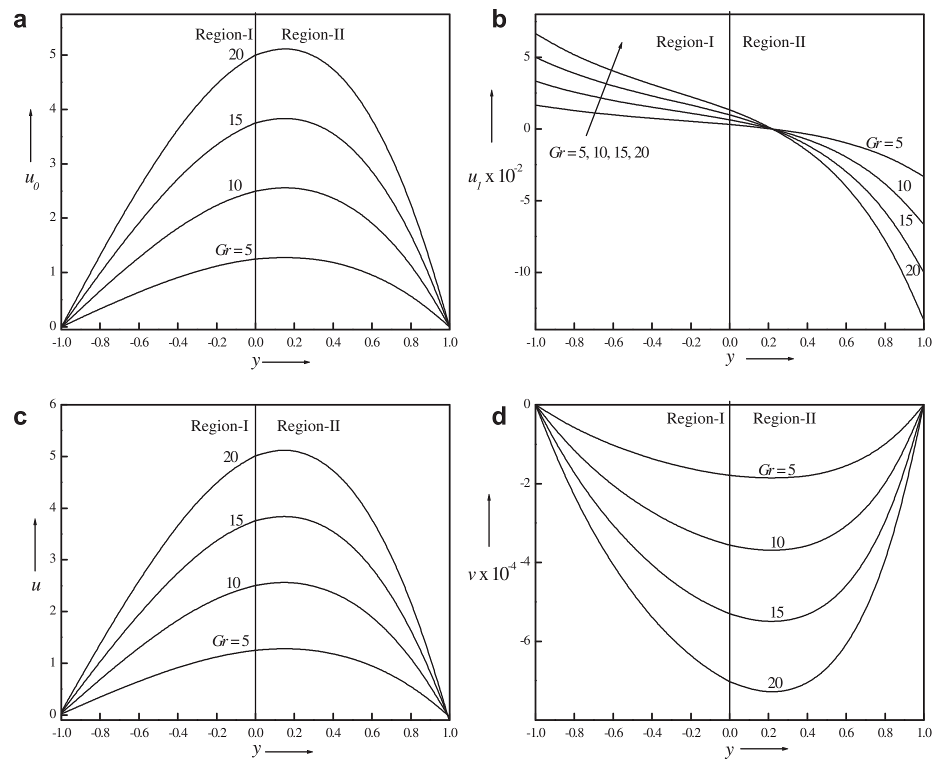

Figure 2 Velocity profiles for different values of Grashof number. (a) zeroth order, (b) first order, (c) total velocity in u and (d) totla velocity in v.

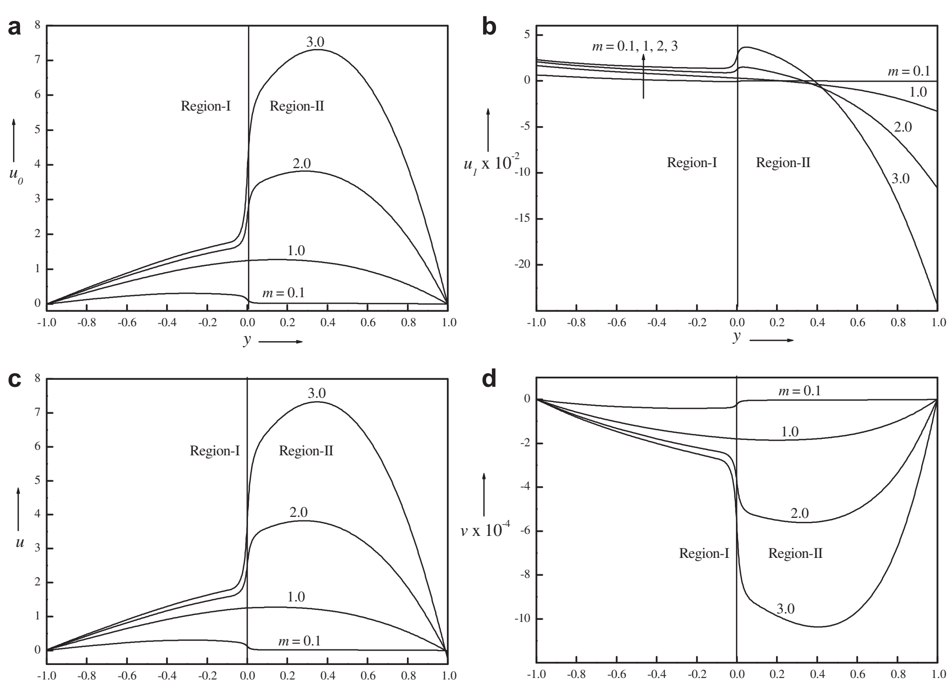

Figure 3 Velocity profiles for different values of viscosity ratio. (a) zeroth order, (b) first order, (c) total velocity in u and (d) totla velocity in v.

viscosity ratio increases to the order of 10^{-3}. The effect of viscosity ratio on the total temperature T is almost identical to that of zeroth order temperature as seen in Fig. 4c.

The effect of width ratio parameter $h(=h^{(2)}/h^{(1)})$ on velocity is similar to the effect of viscosity ratio as shown in Fig. 5. As the width ratio h increases zeroth order velocity

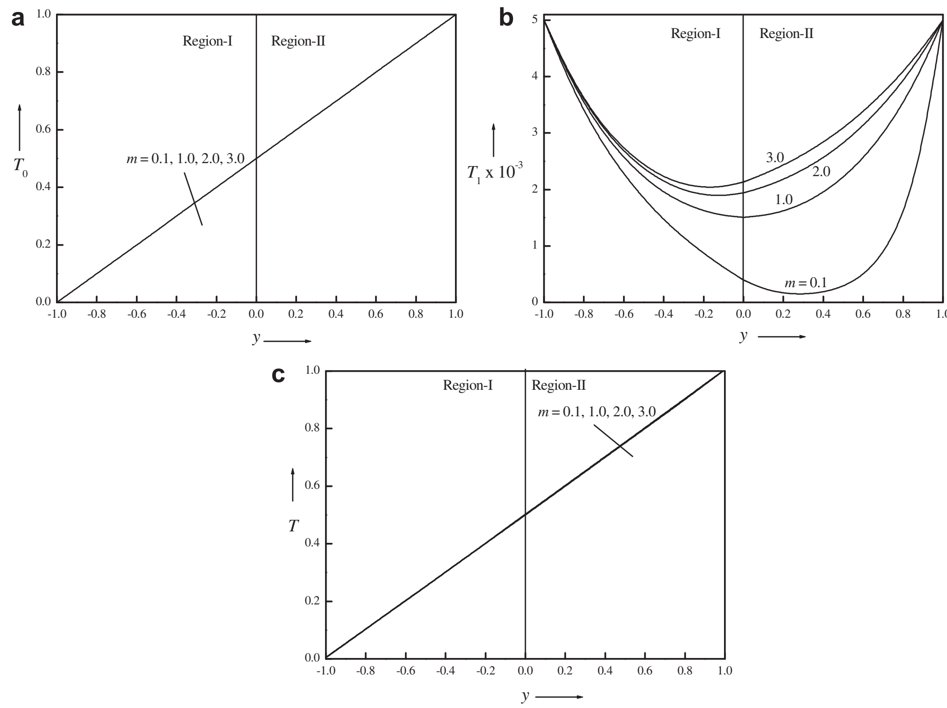

Figure 4 Temperature profiles for different values of viscosity ratio. (a) zeroth order (b) first order and (c) total temperature.

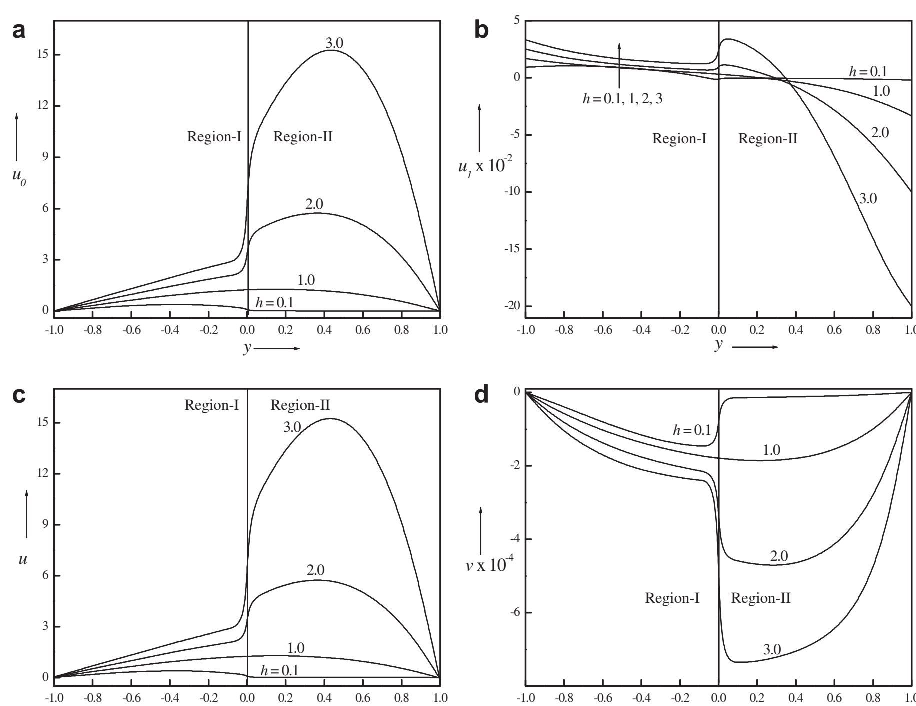

Figure 5 Velocity profiles for different values of width ratio. (a) zeroth order, (b) first order, (c) total velocity in u and (d) total velocity in v.

increases in both the regions, however its effect is more dominant in the region-II compared to region-I as seen in Fig. 5a. The effect of width ratio h on first order velocity u_1 (Fig. 5b) shows that as h increases, u_1 increases from $y = -1$ to $y = 0.4$ approximately while for values of $0.4 \leqslant y \leqslant 1$ the fluid velocity u_1 decreases, and the effect of width ratio is more effective on the right wavy wall as seen in Fig. 5b. It is observed from Fig. 5c that the total fluid velocity u is sim-

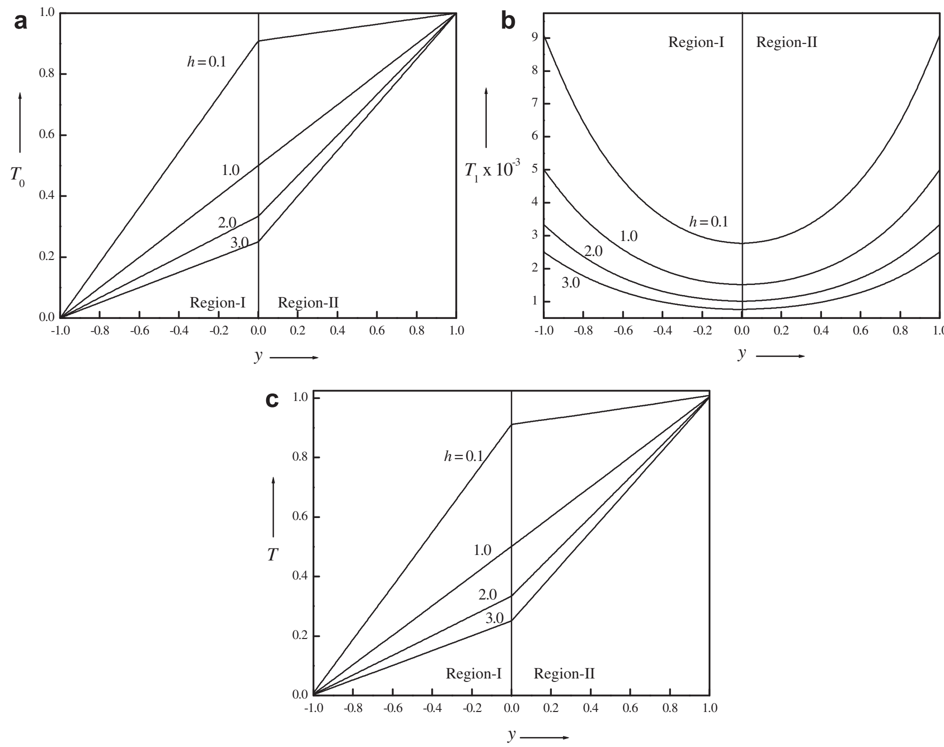

Figure 6 Temperature profiles for different values of width ratio. (a) zeroth order, (b) first order and (c) total temperature.

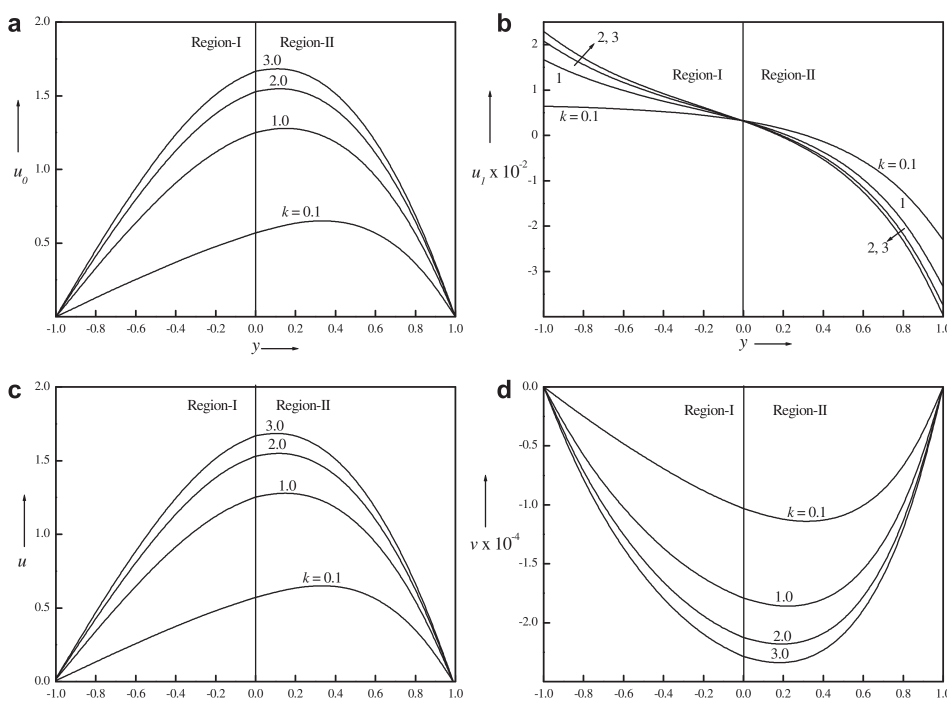

Figure 7 Velocity profiles for different values of conductivity ratio. (a) zeroth order, (b) first order, (c) total velocity in u and (d) total velocity in v.

ilar to that on the zeroth order velocity u_0. The effect of width ratio on velocity v decreases as the width ratio h increases as seen in Fig. 5d.

The effect of width ratio h on the zeroth order temperature is to decrease the temperature in both regions as seen in Fig. 6a. The first order temperature decreases to the order

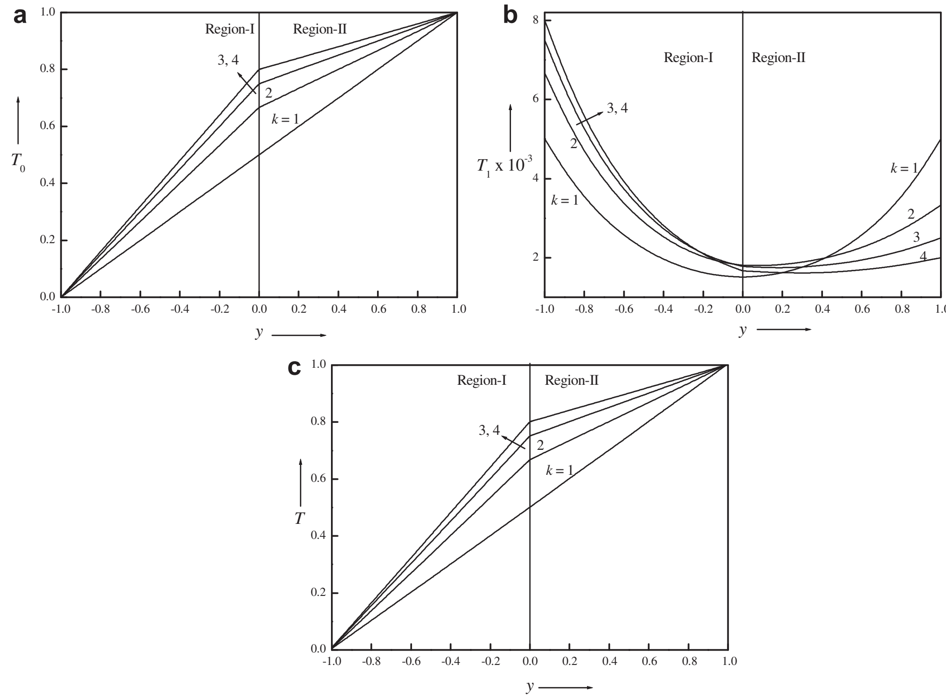

Figure 8 Temperature profiles for different values of conductivity ratio. (a) zeroth order, (b) first order and (c) total temperature.

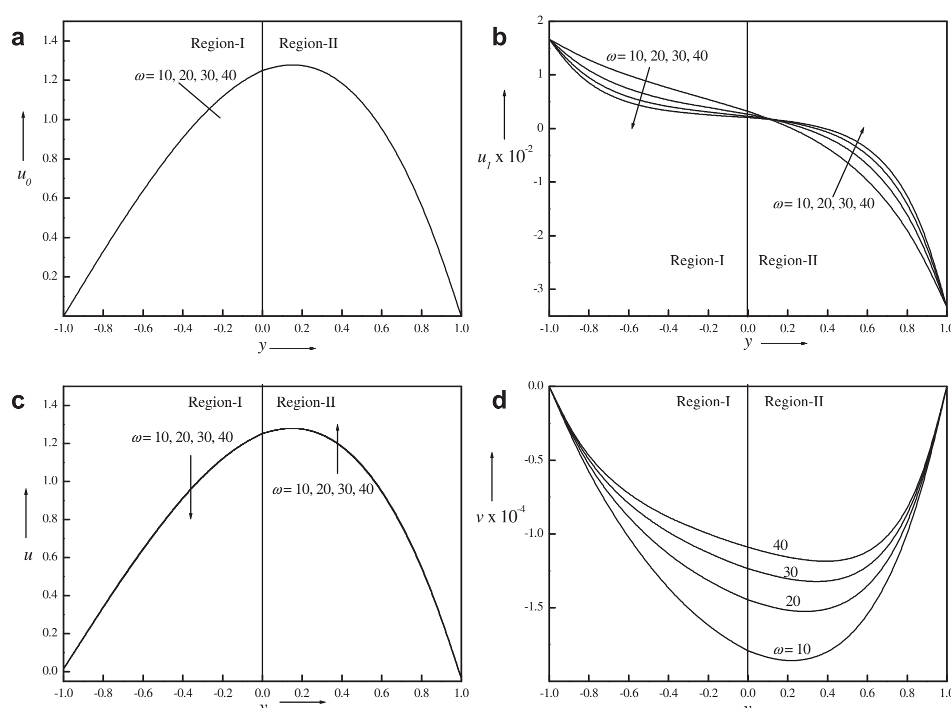

Figure 9 Velocity profiles for different values of frequency parameter. (a) zeroth order, (b) first order, (c) total velocity in u and (d) cross velocity v.

of 10^{-3} in both regions as width ratio h increases as seen in Fig. 6b. The effect of width ratio h on the total temperature T is similar to zeroth order temperature as seen in Fig. 6c.

The effect of conductivity ratio $k(= k^{(2)}/k^{(1)})$ on the velocity is similar to the effect of Grashof number as seen in Fig. 7. Fig. 7a shows that as the conductivity ratio k increases the

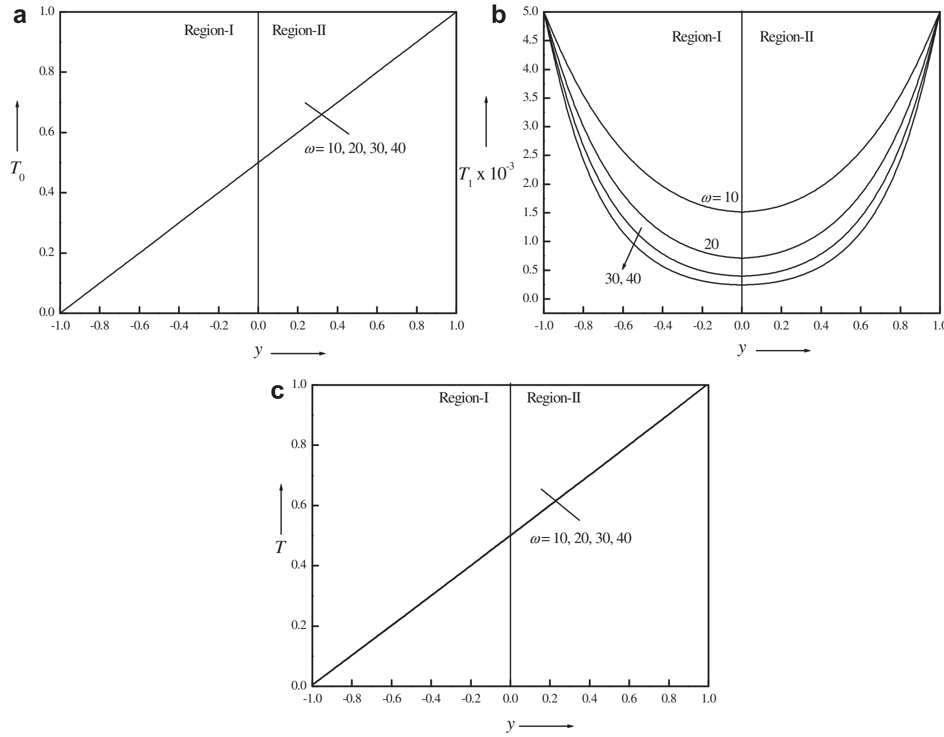

Figure 10 Temperature profiles for different values of frequency parameter. (a) zeroth order, (b) first order and (c) total temperature.

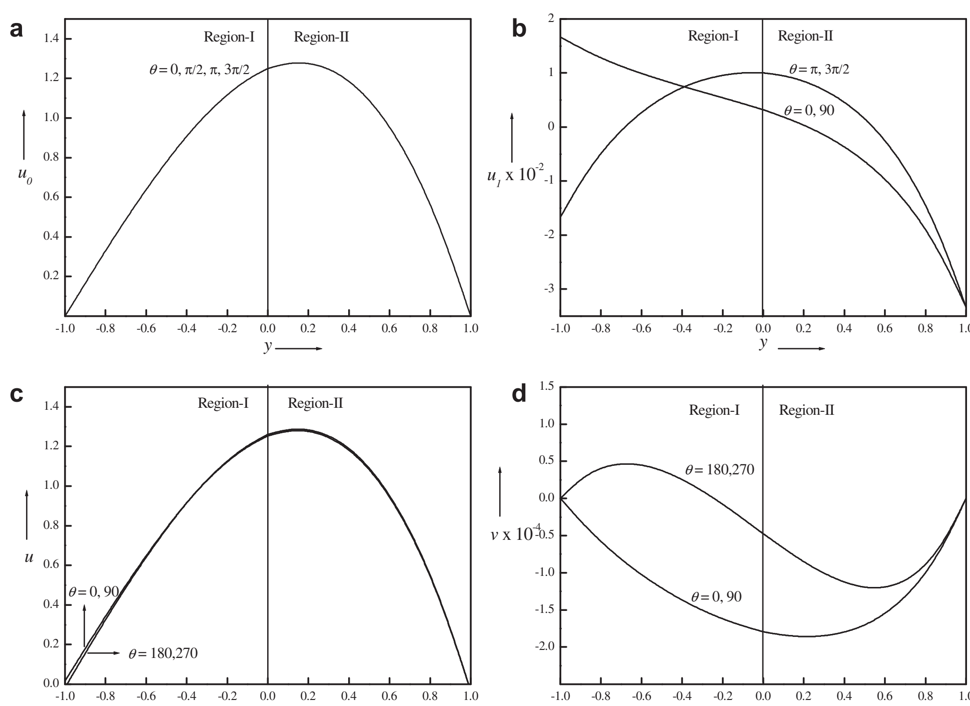

Figure 11 Velocity profiles for different values of traveling thermal temperature θ. (a) zeroth order, (b) first order, (c) total velocity in u and (d) total velocity in v.

zeroth order velocity increase in both the regions. The first order velocity u_1 increases as the conductivity ratio k increases in region-I and decreases in region-II as seen in Fig. 7b. The effect of conductivity ratio k on the total velocity u is similar to the

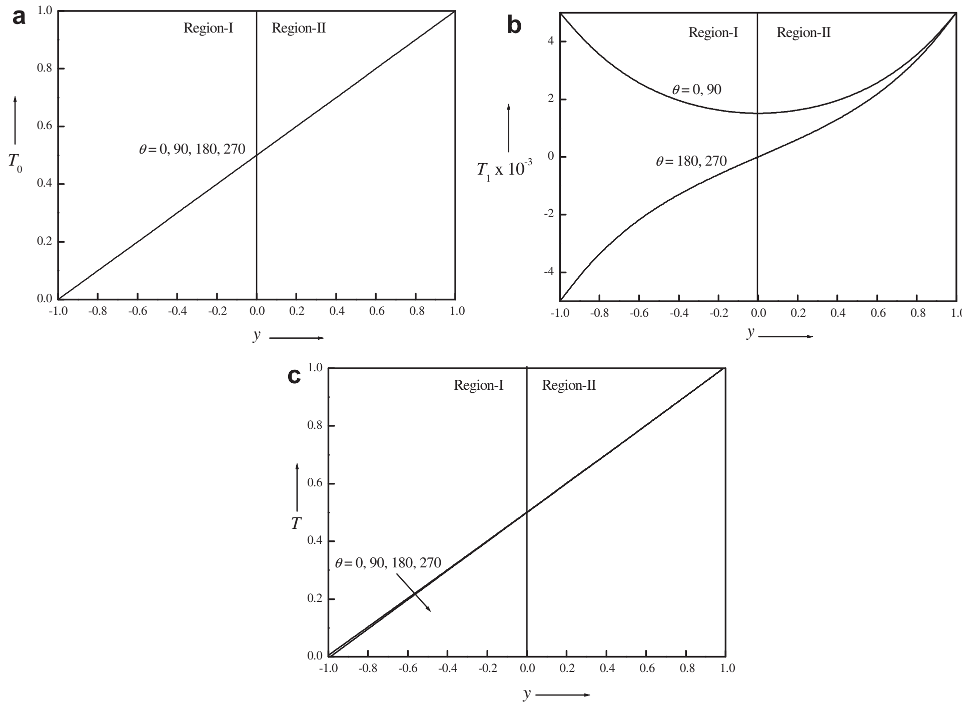

Figure 12 Temperature profiles for different values of traveling thermal temperature θ. (a) zeroth order (b) first order and (c) total temperature.

zeroth order velocity u_0 as seen in Fig. 7c. The behavior of the fluid velocity v perpendicular to the channel length decreases as conductivity ratio k increases as seen in Fig. 7d.

The effect of the conductivity ratio k on zeroth order temperature T_0 is to increase the temperature in both the regions as seen in Fig. 8a. The first order temperature T_1 increases as the conductivity ratio k increases in region-I (i.e. from $y = -1$ to $y = 0.5$ approximately) and decreases from $y = 0.5$ to 1 as seen in Fig. 8b. Here also the effect of conductivity ratio k on total temperature T is similar to the effect on zeroth order temperature.

The effect of the frequency parameter ω on the zeroth order velocity u_0 is invariant as seen in Fig. 9a. The effect of frequency parameter on first order velocity u_1 decreases in region-I ($-1 \leqslant y \leqslant 0$ approximately) and increases in region-II ($0 \leqslant y \leqslant 1$ approximately) as seen in Fig. 9b. There is no effect of the frequency parameter on total velocity u as seen in Fig. 9c. Fig. 9d shows the variations of velocity v perpendicular to the channel length. The velocity v increases as the frequency parameter ω increases to the order of 10^{-4}.

The effect of frequency parameter ω is invariant on zeroth order temperature as seen in Fig. 10a. As the frequency parameter ω increases, the first order temperature decreases in both the regions as seen in Fig. 10b. Here also the effect of frequency parameter ω is invariant on the total temperature as seen in Fig. 10c.

The variations of traveling thermal temperature θ on zeroth order velocity is invariant as seen in Fig. 11a. The first order velocity u_1 decreases near the left wall ($-1 \leqslant y \leqslant -0.4$ approximately) and increases from $y = -0.4$ to 1 (approximately) as

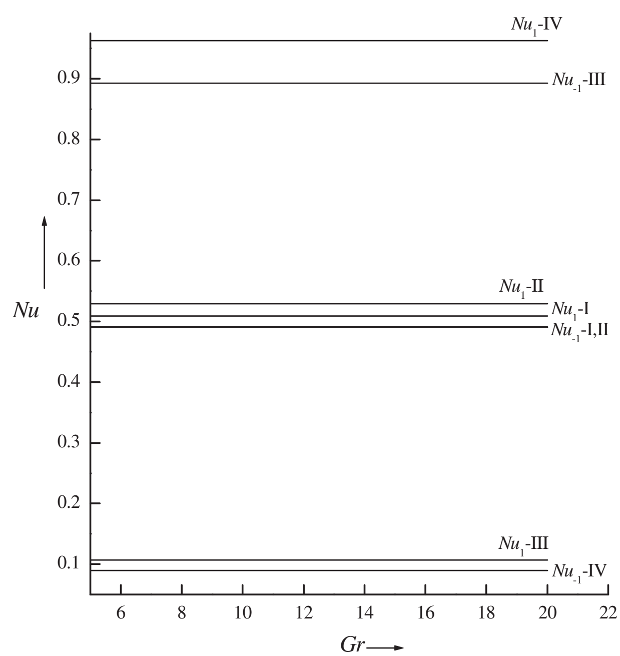

Nusselt number profiles.

	I	II	III	IV
m	1	0.1	1	1
h	1	1	0.1	1
k	1	1	1	0.1

Figure 13 Nusselt number profiles.

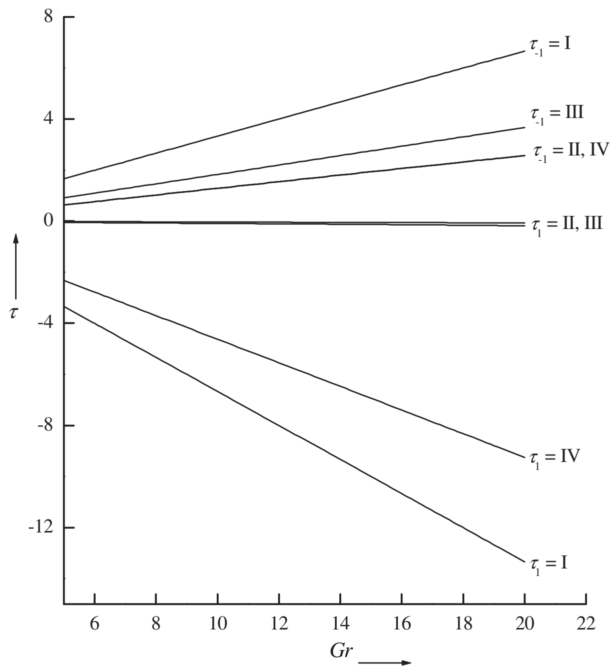

skin friction profiles.

	I	II	III	IV
m	1	0.1	1	1
h	1	1	0.1	1
k	1	1	1	0.1

Figure 14 Skin friction profiles.

traveling thermal temperature θ increases as seen in Fig. 11b. The values for first order velocity u_1 remain the same for $\theta = 0,\pi/2$ and $\pi,3\pi/2$. As the traveling thermal temperature θ increases, total velocity u decreases slightly near the left wall and the effect of traveling thermal temperature is invariant from $y = -0.5$ to 1 as seen in Fig. 11c. Fig. 11d shows the variations of velocity v perpendicular to the channel length. The velocity v increases as traveling thermal temperature θ increases to the order of 10^{-4}. The values for velocity v remain the same for $\theta = 0,\pi/2$ and π, $3\pi/2$.

The variations of traveling thermal temperature θ on zeroth order temperature is invariant as seen in Fig. 12a. Fig. 12b shows the variations of first order temperature. The first order temperature decreases as traveling thermal temperature θ increases to the order of 10^{-3}. Here also the values of $\theta = 0,\pi/2$ and $\pi,3\pi/2$ remain the same as seen in Fig. 12b. There is no effect of traveling thermal temperature θ on total temperature as seen in Fig. 12c.

The Nusselt number Nu is shown in Fig. 13. It is observed that the effect of Grashof number Gr is invariant on Nusselt number. The Nusselt number at the left wavy wall Nu_{-1} is invariant and Nusselt number at the right wavy wall Nu_1 decreases as viscosity ratio m increases. As the width ratio h increases the Nusselt number at the left wall decreases and increases at the right wall. The Nusselt number increases at the left wall and decreases at the right wall as the conductivity ratio k increases.

Fig. 14 shows the behavior of skin friction τ at the channel walls. The effect of increase in Grashof number is to increase the skin friction at the left wall and decreases at the right wall. The effect of viscosity ratio m, width ratio h and conductivity ratio k increases, skin friction increases at the left wall, whereas it decreases at the right wall.

Table 1 shows the variations of temperature on Grashof number. The effect of Grashof number is invariant on zeroth order temperature. As the Grashof number increases first order temperature and total temperature increases to the order of 10^{-4} as seen Table 1.

5. Conclusions

The Grashof number, viscosity ratio, width ratio, and conductivity ratio enhance the velocity parallel to the flow direction and reversal effect is observed on the fluid velocity perpendicular to the channel length. The frequency parameter and traveling thermal temperature is invariant on the velocity parallel to the flow direction and promotes the velocity perpendicular to the flow direction. The Grashof number and viscosity ratio are not operative on the temperature whereas width ratio reduces the temperature and conductivity ratio increases the temperature field. The Nusselt number remains invariant on Grashof number and viscosity ratio whereas the Nusselt number decreases at the left wall and increases at the right wall as width ratio increases and conductivity ratio decreases. The Grashof number, viscosity ratio, width ratio and conductivity ratio promote the skin friction at the left wall and suppresses at the right wall.

Table 1 Temperature values for different values of Grashof number.

y	T_0	T_1			T		
	$Gr = 5,15,20$	$Gr = 5$	$Gr = 15$	$Gr = 20$	$Gr = 5$	$Gr = 15$	$Gr = 20$
−1	0	0.005	0.005	0.005	0.005	0.005	0.005
−0.8	0.1	0.00353	0.00354	0.00354	0.10353	0.10354	0.10354
−0.6	0.2	0.00256	0.00257	0.00257	0.20256	0.20257	0.20257
−0.4	0.3	0.00195	0.00196	0.00197	0.30195	0.30196	0.30197
−0.2	0.4	0.00162	0.00163	0.00163	0.40162	0.40163	0.40163
0	0.5	0.00151	0.00152	0.00153	0.50151	0.50152	0.50153
0.2	0.6	0.00162	0.00163	0.00163	0.60162	0.60163	0.60163
0.4	0.7	0.00195	0.00196	0.00196	0.70195	0.70196	0.70196
0.6	0.8	0.00256	0.00256	0.00257	0.80256	0.80256	0.80257
0.8	0.9	0.00353	0.00353	0.00353	0.90353	0.90353	0.90353
1	1	0.005	0.005	0.005	1.005	1.005	1.005

Acknowledgement

The authors would like to thank the reviewers for their useful suggestions which helped to improve the quality of the paper. We are thankful to the University Grants Commission, New Delhi, India for providing financial assistance to carry out this research work.

Appendix A. Solutions

$$T_0^{(1)} = c_1 y + c_2, \quad T_0^{(2)} = c_3 y + c_4, \quad u_0^{(1)} = l_1 y^3 + l_2 y^2 + d_1 y + d_2, \quad u_0^{(2)} = l_3 y^3 + l_4 y^2 + d_3 y + d_4,$$

$$\phi_{10} = c_5 \cosh(n_1 y) + c_6 \sinh(n_1 y),$$

$$\phi_{20} = c_7 \cosh(n_2 y) + c_8 \sinh(n_2 y),$$

$$\psi_{10} = d_5 + d_6 y + d_7 \cosh(m_1 y) + d_8 \sinh(m_1 y) + l_5 \sinh(n_1 y) + l_6 \cosh(n_1 y),$$

$$\psi_{20} = d_9 + d_{10} y + d_{11} \cosh(m_1 y) + d_{12} \sinh(m_1 y) + l_7 \sinh(n_1 y) + l_8 \cosh(n_1 y),$$

$$\phi_{11} = c_9 \cosh(n_1 y) + c_{10} \sinh(n_1 y) + i(p_1 + p_2 y + p_3 \cosh(m_1 y) + p_4 \sinh(m_1 y) + p_5 y \cosh(n_1 y) + p_6 y \sinh(n_1 y) + p_7 y^2 \times \cosh(n_1 y) + p_8 y^2 \sinh(n_1 y) + p_9 y^3 \cosh(n_1 y) + p_{10} y^3 \times \sinh(n_1 y) + p_{11} y^4 \cosh(n_1 y) + p_{12} y^4 \sinh(n_1 y)),$$

$$\phi_{21} = c_{11} \cosh(n_2 y) + c_{12} \sinh(n_2 y) + i(p_{13} + p_{14} y + p_{15} \times \cosh(m_1 y) + p_{16} \sinh(m_1 y) + p_{17} y \cosh(n_2 y) + p_{18} y \times \sinh(n_2 y) + p_{19} y^2 \cosh(n_2 y) + p_{20} y^2 \sinh(n_2 y) + p_{21} y^3 \times \cosh(n_2 y) + p_{22} y^3 \sinh(n_2 y) + p_{23} y^4 \cosh(n_2 y) + p_{24} y^4 \times \sinh(n_2 y)),$$

$$\psi_{11} = d_{13} + d_{14} y + d_{15} \cosh(m_1 y) + d_{16} \sinh(m_1 y) + i(p_{46} y^2 + p_{47} y^3 + p_{48} y^4 + p_{49} y \cosh(m_1 y) + p_{50} y \sinh(m_1 y) + p_{51} y^2 \cosh(m_1 y) + p_{52} y^2 \sinh(m_1 y) + p_{53} y^3 \cosh(n_1 y) + p_{54} y^3 \sinh(m_1 y) + p_{55} y^4 \cosh(m_1 y) + p_{56} y^4 \sinh(m_1 y) + p_{57} \cosh(n_1 y) + p_{58} \sinh(n_1 y) + p_{59} y \cosh(n_1 y) + p_{60} y \times \sinh(n_1 y) + p_{61} y^2 \cosh(n_1 y) + p_{62} y^2 \sinh(n_1 y) + p_{63} y^3 \times \cosh(n_1 y) + p_{64} y^3 \sinh(n_1 y) + p_{65} y^4 \cosh(n_1 y) + p_{66} y^4 \times \sinh(n_1 y)),$$

$$\psi_{21} = d_{17} + d_{18} y + d_{19} \cosh(m_1 y) + d_{20} \sinh(m_1 y) + i(f_{22} y^2 + f_{23} y^3 + f_{24} y^4 + f_{25} y \cosh(m_1 y) + f_{26} y \sinh(m_1 y) + f_{27} y^2 \times \cosh(m_1 y) + f_{28} y^2 \sinh(m_1 y) + f_{29} y^3 \cosh(n_1 y) + f_{30} y^3 \times \sinh(m_1 y) + f_{31} y^4 \cosh(m_1 y) + f_{32} y^4 \sinh(m_1 y) + f_{33} \times \cosh(n_2 y) + f_{34} \sinh(n_2 y) + f_{35} y \cosh(n_2 y) + f_{36} y \times \sinh(n_2 y) + f_{37} y^2 \cosh(n_2 y) + f_{38} y^2 \sinh(n_2 y) + f_{39} y^3 \times \cosh(n_2 y) + f_{40} y^3 \sinh(n_2 y) + f_{41} y^4 \cosh(n_2 y) + f_{42} y^4 \times \sinh(n_2 y)).$$

$$A = Gr\beta h^3 m^2 r^2; \quad c_1 = -\frac{h}{k+h}, \quad c_3 = \frac{hc_1}{k},$$

$$c_4 = 1 + c_3, \quad c_2 = c_4, \quad l_1 = -\frac{Grc_1}{6}, \quad l_2 = -\frac{Grc_2}{2},$$

$$l_3 = -\frac{Ac_3}{6}, \quad l_4 = -\frac{Ac_4}{2}, \quad d_1 = \frac{d_3}{m^2 h^2 r}, \quad d_2 = \frac{d_4}{mhr},$$

$$d_3 = \frac{(l_4 - l_3)mh - (l_1 + l_2)m^2 h^2 r}{mh + 1},$$

$$d_4 = d_3 + l_3 - l_4, \quad n_1 = \sqrt{\frac{\omega \Pr}{2}}(1+i),$$

$$n_2 = \sqrt{\frac{\omega \Pr}{2km}}(1+i), \quad c_5 = c_7, \quad c_6 = \frac{kn_2 c_8}{hn_1},$$

$$c_7 = \frac{hc_8 \sinh(n_2) - \cos(\omega t - \theta)c_3}{h \cosh(n_2)},$$

$$c_8 = \frac{n_1 c_3 \cos(\omega t - \theta)\cosh(n_1) - n_1 hc_1 \cos(\omega t)\cosh(n_2)}{kn_2 \sinh(n_1)\cosh(n_2) + n_1 h \sinh(n_2)\cosh(n_1)},$$

$$m_1 = \sqrt{\frac{\omega}{2}}(1+i), \quad l_5 = \frac{Grc_5}{n_1(n_1^2 - m_1^2)}, \quad l_6 = \frac{Grc_6}{n_1(n_1^2 - m_1^2)},$$

$$l_7 = \frac{Ac_7}{n_2(n_2^2 - m_1^2)}, \quad l_8 = \frac{Ac_8}{n_2(n_2^2 - m_1^2)},$$

$$z_1 = l_5 \sinh(n_1) + l_6 \cosh(n_1),$$

$$z_2 = l_5 n_1 \cosh(n_1) + n_1 l_6 \sinh(n_1) - \cos(\omega t)(3l_1 + 2l_2 + d_1),$$

$$z_3 = l_8 \cosh(n_2) - l_7 \sinh(n_2),$$

$$z_4 = l_7 n_2 \cosh(n_2) - n_2 l_8 \sinh(n_2) - \frac{\cos(\omega t - \theta)}{h}(3l_3 - 2l_4 + d_3), \quad z_5 = m_1 r m^2 h^3,$$

$$z_6 = \frac{1}{z_5}(rm^2 h^3 (n_1^3 l_5 - Grc_5 - m_1^2 n_1 l_5) - n_2^3 l_7 + Ac_7 + m_1^2 n_2 l_7), \quad z_7 = \frac{1}{rm^2 h^2},$$

$$z_8 = \frac{n_2^2 l_8}{m_1^2 rm^2 h^2} - \frac{n_1^2 l_6}{m_1^2}, \quad z_9 = \frac{1}{m_1 rmh} - \frac{m_1}{z_5}, \quad z_{10} = \frac{1}{rmh},$$

$$z_{11} = \frac{1}{m_1}(z_{10} n_2 l_7 - z_6 - n_1 l_5),$$

$$z_{12} = z_{10} - z_7, \quad z_{13} = z_{10} l_8 - z_8 - l_6,$$

$$z_{14} = z_9 \sinh(m_1) + \frac{m_1^2}{z_5}, \quad z_{15} = z_{12} + z_7 \cosh(m_1),$$

$$z_{16} = z_{10} \sinh(m_1),$$

$$z_{17} = z_{13} + z_6 + z_1 + z_8 \cosh(m_1) + z_{11} \sinh(m_1),$$

$$z_{18} = \frac{m_1^2}{z_5} + m_1 z_5 \cosh(m_1), \quad z_{19} = m_1 z_7 \sinh(m_1),$$

$$z_{20} = m_1 z_{10} \cosh(m_1),$$

$$z_{21} = z_6 + z_2 + z_8 m_1 \sinh(m_1) + z_{11} m_1 \cosh(m_1),$$

$$z_{22} = z_{10} + z_{14}, \quad z_{23} = z_{15} - z_{10} \cosh(m_1),$$

$$z_{24} = z_{16} + z_{10} \sinh(m_1), \quad z_{25} = z_{17} - z_3 z_{10},$$

$$z_{26} = z_{19} + z_{18} m_1 \sinh(m_1),$$

$$z_{27} = z_{20} - m_1 z_{18} \cosh(m_1), \quad z_{28} = z_{21} - z_4 z_{18},$$

$$z_{29} = z_{23} + z_{22} m_1 \sinh(m_1),$$

$z_{30} = z_{24} - m_1 z_{22}\cosh(m_1), \quad z_{31} = z_{25} - z_4 z_{22},$

$$d_{12} = \frac{z_{26}z_{31} - z_{28}z_{29}}{z_{27}z_{29} - z_{26}z_{30}}, \quad d_{11} = \frac{-z_{28} - z_{27}d_{12}}{z_{26}},$$

$d_{10} = m_1 d_{11}\sinh(m_1) - m_1 d_{12}\cosh(m_1) - z_4,$
$d_9 = d_{10} - d_{11}\cosh(m_1) + d_{12}\sinh(m_1) - z_3,$
$d_8 = z_9 d_{10} + z_{10} d_{12} + z_{11}, \quad d_7 = z_7 d_{11} + z_8,$

$$d_6 = \frac{m_1^2 d_{10}}{z_5} + z_6, \quad d_5 = z_{10}d_9 + z_{12}d_{11} + z_{13},$$

$$p_1 = -\frac{\mathrm{Pr}c_1 d_5}{n_1^2}, \quad p_2 = -\frac{\mathrm{Pr}c_1 d_6}{n_1^2}, \quad p_3 = \frac{\mathrm{Pr}c_1 d_7}{m_1^2 - n_1^2},$$
$$p_4 = \frac{\mathrm{Pr}c_1 d_8}{m_1^2 - n_1^2},$$

$$p_5 = \mathrm{Pr}\left(\frac{c_6 d_6 + c_1 l_5}{2n_1} - \frac{c_5 d_1}{4n_1^2} + \frac{l_2 c_6}{4n_1^3} - \frac{3l_1 c_5}{8n_1^4}\right),$$
$$p_6 = \mathrm{Pr}\left(\frac{c_5 d_2 + c_1 l_6}{2n_1} - \frac{c_6 d_1}{4n_1^2} + \frac{l_2 c_5}{4n_1^3} - \frac{3l_1 c_6}{8n_1^4}\right),$$

$$p_7 = \mathrm{Pr}\left(\frac{c_6 d_1}{4n_1} - \frac{l_2 c_5}{4n_1^2} + \frac{3l_1 c_6}{8n_1^3}\right),$$
$$p_8 = \mathrm{Pr}\left(\frac{c_5 d_1}{4n_1} - \frac{l_2 c_6}{4n_1^2} + \frac{3l_1 c_5}{8n_1^3}\right), \quad p_9 = \mathrm{Pr}\left(\frac{l_2 c_6}{6n_1} - \frac{l_1 c_5}{4n_1^2}\right),$$

$$p_{10} = \mathrm{Pr}\left(\frac{l_2 c_5}{6n_1} - \frac{l_1 c_6}{4n_1^2}\right), \quad p_{11} = -\frac{\mathrm{Pr}c_6 l_1}{8n_1}, \quad p_{12} = -\frac{\mathrm{Pr}c_5 l_1}{8n_1},$$
$$P = \frac{\mathrm{Pr}}{km}, \quad p_{13} = -\frac{Pc_3 d_9}{n_2^2},$$

$$p_{14} = -\frac{Pc_3 d_{10}}{n_2^2}, \quad p_{15} = \frac{Pc_3 d_{10}}{m_1^2 - n_2^2}, \quad p_{16} = \frac{Pc_3 d_{12}}{m_1^2 - n_2^2},$$
$$p_{16} = P\left(\frac{c_8 d_4 + c_3 l_7}{2n_2} - \frac{c_7 d_3}{4n_2^2} + \frac{l_4 c_8}{4n_2^3} - \frac{3l_3 c_7}{8n_2^4}\right),$$

$$p_{17} = P\left(\frac{c_8 d_4 + c_3 l_7}{2n_2} - \frac{c_7 d_3}{4n_2^2} + \frac{l_4 c_8}{4n_2^3} - \frac{3l_3 c_7}{8n_2^4}\right),$$
$$p_{18} = P\left(\frac{c_7 d_4 + c_3 l_8}{2n_2} - \frac{c_8 d_3}{4n_2^2} + \frac{l_4 c_7}{4n_2^3} - \frac{3l_3 c_8}{8n_2^4}\right),$$

$$p_{19} = P\left(\frac{c_8 d_3}{4n_2} - \frac{l_4 c_7}{4n_2^2} + \frac{3l_3 c_8}{8n_2^3}\right),$$
$$p_{20} = P\left(\frac{c_7 d_3}{4n_2} - \frac{l_4 c_8}{4n_2^2} + \frac{3l_3 c_7}{8n_2^3}\right), \quad p_{21} = P\left(\frac{l_4 c_8}{6n_2} - \frac{l_3 c_7}{4n_2^2}\right),$$

$$p_{22} = P\left(\frac{l_4 c_7}{6n_2} - \frac{l_3 c_8}{4n_2^2}\right), \quad p_{23} = \frac{Pl_3 c_8}{8n_2}, \quad p_{24} = \frac{Pl_3 c_7}{8n_2},$$

$$z_{32} = p_1 + p_2 + p_3\cosh(m_1) + p_4\sinh(m_1) + (p_5 + p_7 + p_9 + p_{11})\cosh(n_1) + (p_6 + p_8 + p_{10} + p_{12})\sinh(n_1),$$

$$z_{33} = p_{13} - p_{14} + p_{15}\cosh(m_1) - p_{16}\sinh(m_1) + (p_{19} - p_{17} - p_{21} + p_{23})\cosh(n_2) + (p_{18} - p_{20} + p_{22} - p_{24})\sinh(n_2),$$

$$z_{34} = p_{13} + p_{15} - p_1 - p_3, \quad z_{35} = \frac{1}{n_1}\left(\frac{k}{h}(p_{14} + m_1 p_{16} + p_{17} + c_7) - p_2 - m_1 p_4 - p_5 - c_5\right),$$

$$z_{36} = z_{32} + z_{34}\cosh(n_1) + z_{35}\sinh(n_1), \quad c_9 = c_{11} + iz_{34}, \quad c_{10} = \frac{kn_2 c_{12}}{hn_1} + iz_{35},$$
$$c_{11} = \frac{c_{12}\sinh(n_2) - z_{33}}{\cosh(n_2)},$$
$$c_{12} = \frac{ihn_1(z_{33}\cosh(n_1) - z_{36}\cosh(n_2))}{kn_2\sinh(n_1)\cosh(n_2) + hn_1\sinh(n_2)\cosh(n_1)},$$

$p_{25} = Grp_2 - 2l_2 d_5, \quad p_{26} = -6l_1 d_5 - 2l_2 d_6, \quad p_{27} = -6l_1 d_6,$
$p_{28} = d_2 d_7 m_1^2 - 2l_2 d_7 + Grm_1 p_4,$

$p_{29} = d_2 d_8 m_1^2 - 2l_2 d_8 + Grm_1 p_3, \quad p_{30} = d_1 d_7 m_1^2 - 6l_1 d_7,$
$p_{31} = d_1 d_8 m_1^2 - 6l_1 d_8, \quad p_{32} = l_2 d_7 m_1^2,$

$p_{33} = l_2 d_8 m_1^2, \quad p_{34} = l_1 d_7 m_1^2, \quad p_{35} = l_1 d_8 m_1^2,$
$p_{36} = d_2 l_6 n_1^2 - 2l_2 l_6 + Gr(p_5 + n_1 c_{10}),$

$p_{37} = d_2 l_5 n_1^2 - 2l_2 l_5 + Gr(p_6 + n_1 c_9),$
$p_{38} = d_1 l_6 n_1^2 - 6l_1 l_6 + Gr(n_1 p_6 + 2p_7),$

$p_{39} = d_1 l_5 n_1^2 - 6l_1 l_5 + Gr(n_1 p_5 + 2p_8),$
$p_{40} = l_2 l_6 n_1^2 + Gr(n_1 p_8 + 3p_9),$

$p_{41} = l_2 l_5 n_1^2 + Gr(n_1 p_7 + 3p_{10}),$
$p_{42} = l_1 l_6 n_1^2 + Gr(n_1 p_{10} + 4p_{11}),$

$p_{43} = l_1 l_5 n_1^2 + Gr(n_1 p_9 + 4p_{12}), \quad p_{44} = Grn_1 p_{12},$
$p_{45} = Grn_1 p_{11}, \quad a_1 = n_1^4 - n_1^2 m_1^2,$

$a_2 = 4n_1^3 - 2n_1 m_1^2, \quad a_3 = 6n_1^2 - m_1^2, \quad a_4 = 4n_1,$

$$p_{46} = -\frac{p_{25}}{2m_1^2} - \frac{p_{27}}{m_1^4}, \quad p_{47} = -\frac{p_{26}}{6m_1^2},$$

$$p_{48} = -\frac{p_{27}}{12m_1^2}, \quad p_{49} = \frac{p_{29}}{2m_1^3} - \frac{5p_{30}}{4m_1^4} + \frac{17p_{33}}{4m_1^5} - \frac{147p_{34}}{8m_1^6},$$
$$p_{50} = \frac{p_{28}}{2m_1^3} - \frac{5p_{32}}{4m_1^4} + \frac{17p_{32}}{4m_1^5} - \frac{147p_{35}}{8m_1^6},$$
$$p_{51} = \frac{p_{31}}{4m_1^3} - \frac{5p_{32}}{4m_1^4} + \frac{51p_{35}}{8m_1^5}, \quad p_{52} = \frac{p_{30}}{4m_1^3} - \frac{5p_{33}}{4m_1^4} + \frac{51p_{34}}{8m_1^5},$$
$$p_{53} = \frac{p_{33}}{6m_1^3} - \frac{5p_{34}}{4m_1^4},$$

$$p_{54} = \frac{p_{32}}{6m_1^3} - \frac{5p_{35}}{4m_1^4}, \quad p_{55} = \frac{p_{35}}{2m_1^3}, \quad p_{56} = \frac{p_{34}}{2m_1^3},$$
$$p_{57} = \frac{p_{36}}{a_1} - \frac{a_2 p_{39}}{a_1^2} + p_{40}\left(\frac{2a_2^2}{a_1^3} - \frac{2a_3}{a_1^2}\right) - p_{43}\left(\frac{6a_4}{a_1^2} - \frac{12a_2 a_3}{a_1^3} + \frac{6a_2^3}{a_1^4}\right) - p_{44}\left(\frac{24}{a_1^2} - \frac{24a_3^2}{a_1^3} + \frac{72a_2^2 a_3}{a_1^4} - \frac{24a_2^4}{a_1^5}\right)$$

$$p_{58}=\frac{p_{37}}{a_1}-\frac{a_2p_{38}}{a_1^2}+p_{41}\left(\frac{2a_2^2}{a_1^3}-\frac{2a_3}{a_1^2}\right)-p_{42}\left(\frac{6a_4}{a_1^2}-\frac{12a_2a_3}{a_1^3}+\frac{6a_2^3}{a_1^4}\right)-p_{45}\left(\frac{24}{a_1^2}-\frac{24a_3^2}{a_1^3}+\frac{72a_2^2a_3}{a_1^4}-\frac{24a_2^4}{a_1^5}\right),$$

$$p_{59}=\frac{p_{38}}{a_1}-\frac{2a_2p_{41}}{a_1^2}-p_{42}\left(\frac{6a_3}{a_1^2}-\frac{6a_2^2}{a_1^3}\right)-p_{45}\left(\frac{24a_4}{a_1^2}-\frac{48a_2a_3}{a_1^3}+\frac{24a_2^3}{a_1^4}\right),$$

$$p_{60}=\frac{p_{39}}{a_1}-\frac{2a_2p_{40}}{a_1^2}-p_{43}\left(\frac{6a_3}{a_1^2}-\frac{6a_2^2}{a_1^3}\right)-p_{44}\left(\frac{24a_4}{a_1^2}-\frac{48a_2a_3}{a_1^3}+\frac{24a_2^3}{a_1^4}\right),$$

$$p_{61}=\frac{p_{40}}{a_1}-\frac{3a_2p_{43}}{a_1^2}-p_{44}\left(\frac{12a_3}{a_1^2}-\frac{12a_2^2}{a_1^3}\right),$$
$$p_{62}=\frac{p_{41}}{a_1}-\frac{3a_2p_{42}}{a_1^2}-p_{45}\left(\frac{12a_3}{a_1^2}-\frac{12a_2^2}{a_1^3}\right),$$

$$p_{63}=\frac{p_{42}}{a_1}-\frac{4a_2p_{45}}{a_1^2},\quad p_{64}=\frac{p_{43}}{a_1}-\frac{4a_2p_{44}}{a_1^2},$$
$$p_{65}=\frac{p_{44}}{a_1},\quad p_{66}=\frac{p_{45}}{a_1},\quad f_1=Ap_{14}-2l_4d_9,$$

$$f_2=-6l_3d_9-2l_4d_{10},\quad f_3=-6l_3d_{10},$$
$$f_4=d_4d_{11}m_1^2-2l_4d_{11}+Am_1p_{16},$$

$$f_5=d_4d_{12}m_1^2-2l_4d_{12}+Am_1p_{15},\quad f_6=d_3d_{11}m_1^2-6l_3d_{11},$$
$$f_7=d_3d_{12}m_1^2-6l_3d_{12},\quad f_8=l_4d_{11}m_1^2,$$

$$f_9=l_4d_{12}m_1^2,\quad f_{10}=l_3d_{11}m_1^2,\quad f_{11}=l_3d_{12}m_1^2,$$
$$f_{12}=d_4l_8n_2^2-2l_4l_8+A(p_{17}+n_2c_{12}),$$

$$f_{13}=d_4l_7n_2^2-2l_4l_7+A(p_{18}+n_2c_{11}),$$
$$f_{14}=d_3l_8n_2^2-6l_3l_8+A(n_2p_{18}+2p_{19}),$$

$$f_{15}=d_3l_7n_2^2-6l_3l_7+A(n_2p_{17}+2p_{20}),$$
$$f_{16}=l_4l_8n_2^2+A(n_2p_{20}+3p_{21}),$$

$$f_{17}=l_4l_7n_2^2+A(n_2p_{19}+3p_{22}),\quad f_{18}=l_3l_8n_2^2+A(n_2p_{22}+4p_{23}),$$

$$f_{19}=l_3l_7n_2^2+A(n_2p_{21}+4p_{24}),\quad f_{20}=An_2p_{24},$$
$$f_{21}=An_2p_{23},\quad b_1=n_2^4-n_2^2m_1^2,$$

$$b_2=4n_2^3-2n_2m_1^2,\quad b_3=6n_2^2-m_1^2,\quad b_4=4n_2,$$
$$f_{22}=-\frac{f_1}{2m_1^2}-\frac{f_3}{m_1^4},\quad f_{23}=-\frac{f_2}{6m_1^2},\quad f_{24}=-\frac{f_3}{12m_1^2},$$

$$f_{25}=\frac{f_5}{2m_1^3}-\frac{5f_6}{4m_1^4}+\frac{17f_9}{4m_1^5}-\frac{147f_{10}}{8m_1^6},$$
$$f_{26}=\frac{f_4}{2m_1^3}-\frac{5f_7}{4m_1^4}+\frac{17f_8}{4m_1^5}-\frac{147f_{11}}{8m_1^6},$$

$$f_{27}=\frac{f_7}{4m_1^3}-\frac{5f_8}{4m_1^4}+\frac{51f_{11}}{8m_1^5},\quad f_{28}=\frac{f_6}{4m_1^3}-\frac{5f_9}{4m_1^4}+\frac{51f_{10}}{8m_1^5},$$
$$f_{29}=\frac{f_9}{4m_1^3}-\frac{5f_{10}}{2m_1^4},\quad f_{30}=\frac{f_8}{4m_1^3}-\frac{5f_{11}}{2m_1^4},$$

$$f_{31}=\frac{f_{11}}{2m_1^3},\quad f_{32}=\frac{f_{10}}{2m_1^3},\quad f_{33}=\frac{f_{12}}{b_1}-\frac{b_2f_{15}}{b_1^2}+f_{10}\left(\frac{2b_2^2}{b_1^3}-\frac{2b_3}{b_1^2}\right)-f_{19}\left(\frac{6b_4}{b_1^2}-\frac{12b_2b_3}{b_1^3}+\frac{6b_2^3}{b_1^4}\right)-f_{20}\left(\frac{24}{b_1^2}-\frac{24b_3^2}{b_1^3}+\frac{72b_2^2b_3}{b_1^4}-\frac{24b_2^4}{b_1^5}\right),$$

$$f_{34}=\frac{f_{13}}{b_1}-\frac{b_2f_{14}}{b_1^2}+f_{17}\left(\frac{2b_2^2}{b_1^3}-\frac{2b_3}{b_1^2}\right)-f_{18}\left(\frac{6b_4}{b_1^2}-\frac{12b_2b_3}{b_1^3}+\frac{6b_2^3}{b_1^4}\right)-f_{21}\left(\frac{24}{b_1^2}-\frac{24b_3^2}{b_1^3}+\frac{72b_2^2b_3}{b_1^4}-\frac{24b_2^4}{b_1^5}\right),$$

$$f_{35}=\frac{f_{14}}{b_1}-\frac{2b_2f_{17}}{b_1^2}+f_{18}\left(\frac{6b_2^2}{b_1^3}-\frac{6b_3}{b_1^2}\right)-f_{21}\left(\frac{24b_4}{b_1^2}-\frac{48b_2b_3}{b_1^3}+\frac{24b_2^3}{b_1^4}\right),$$

$$f_{36}=\frac{f_{15}}{b_1}-\frac{2b_2f_{16}}{b_1^2}+f_{19}\left(\frac{6b_2^2}{b_1^3}-\frac{6b_3}{b_1^2}\right)-f_{20}\left(\frac{24b_4}{b_1^2}-\frac{48b_2b_3}{b_1^3}+\frac{24b_2^3}{b_1^4}\right),$$

$$f_{37}=\frac{f_{16}}{b_1}-\frac{3b_2f_{19}}{b_1^2}+f_{20}\left(\frac{12b_2^2}{b_1^3}-\frac{12b_3}{b_1^2}\right),$$
$$f_{38}=\frac{f_{17}}{b_1}-\frac{3b_2f_{18}}{b_1^2}+f_{21}\left(\frac{12b_2^2}{b_1^3}-\frac{12b_3}{b_1^2}\right),$$

$$f_{39}=\frac{f_{18}}{b_1}-\frac{4b_2f_{21}}{b_1^2},\quad f_{40}=\frac{f_{19}}{b_1}-\frac{4b_2f_{20}}{b_1^2},\quad f_{41}=\frac{f_{20}}{b_1},\quad f_{42}=\frac{f_{21}}{b_1},$$
$$z_{37}=p_{46}+p_{47}+p_{48}+(p_{49}+p_{51}+p_{53}+p_{55})\cosh(m_1)+(p_{50}+p_{52}+p_{54}+p_{56})\sinh(m_1)+(p_{57}+p_{59}+p_{61}+p_{63}+p_{65})\cosh(n_1)+(p_{58}+p_{60}+p_{62}+p_{64}+p_{66})\sinh(n_1),$$

$$z_{38}=2p_{46}+3p_{47}+4p_{48}+(p_{49}+m_1p_{50}+2p_{51}+m_1p_{52}+3p_{53}+4p_{55}+m_1p_{56})\cosh(m_1)+(p_{50}+m_1p_{49}+2p_{52}+m_1p_{51}+3p_{54}+m_1p_{53}+4p_{56}+m_1p_{55})\sinh(m_1)+(n_1p_{58}+p_{59}+n_1p_{60}+2p_{61}+n_1p_{62}+3p_{63}+n_1p_{64}+4p_{65}+n_1p_{66})\times\cosh(n_1)+(n_1p_{57}+n_1p_{59}+p_{60}+n_1p_{61}+2p_{62}+n_1p_{63}+3p_{64}+n_1p_{65}+4p_{66})\sinh(n_1),$$

Primary categories of fluid flow interface conditions between fluid-fluid and porous-fluid layers.

Model	Velocity	Temperature
Model 1	$u_p = u_f;\quad \left(\frac{du}{dy}\right)_p = \left(\frac{du}{dy}\right)_f$ Jang and Chen (1992).	$T_p = T_f;\quad K_{eff}\frac{\partial T_f}{\partial y} = K_f\frac{\partial T_p}{\partial y}$ Kuznetsov (1999)
Model 2	$u_p = u_f;\quad \mu_{eff}\left(\frac{du}{dy}\right)_p = \mu\left(\frac{du}{dy}\right)_f$ Kim and Choi (1996).	$T_p = T_f;\quad \phi + K_f\left(\frac{\partial T}{\partial y}\right)_f = K_{eff}\left(\frac{\partial T}{\partial y}\right)_p$ Ochoa-Tapia and Whitaker (1998a).
Model 3	$u_p = u_f;\quad \frac{\mu}{\varepsilon}\left(\frac{du}{dy}\right)_p - \mu\left(\frac{du}{dy}\right)_f = \beta_1\frac{\mu}{\sqrt{K}}u$ Kuznetsov (1999).	$\left(\frac{dT}{dy}\right)_p = \frac{\alpha_T}{\lambda}(T_p - T_f); K_{eff}\frac{\partial T_f}{\partial y} = K_f\frac{\partial T_p}{\partial y}$ Sahraoui and Kaviany (1994)
Model 4	$u_p = u_f;\quad \frac{\mu}{\varepsilon}\left(\frac{du}{dy}\right)_p - \mu\left(\frac{du}{dy}\right)_f = \beta_1\frac{\mu}{\sqrt{K}}u + \beta_2\rho u^2$ Ochoa-Tapia and Whitaker (1998b).	$\left(\frac{dT}{dy}\right)_p = \frac{\alpha_T}{\lambda}(T_p - T_f);\quad K_{eff}\frac{\partial T_f}{\partial y} = K_f\frac{\partial T_p}{\partial y}$ Sahraoui and Kaviany (1994)
Model 5	$\left(\frac{du}{dy}\right)_f = \frac{\alpha^*}{\sqrt{K}}(u_{int} - u_\infty)$ Sahraoui and Kaviany (1992).	

$$z_{39} = f_{22} - f_{23} + f_{24} + (f_{27} - f_{25} - f_{29} + f_{31})\cosh(m_1) + (f_{26} - f_{28} + f_{30} - f_{32})\sinh(m_1) + (f_{33} - f_{35} + f_{37} - f_{39} + f_{41}) \times \cosh(n_2) + (f_{36} - f_{34} - f_{38} + f_{40} - f_{42})\sinh(n_2),$$

$$z_{40} = -2f_{22} + 3f_{23} - 4f_{24} + (f_{25} - 2f_{27} + 3f_{29} - 4f_{31} - m_1f_{26} + m_1f_{28} - m_1f_{30} + m_1f_{32})\cosh(m_1) + (-f_{26} + 2f_{28} - 3f_{30} + 4f_{32} - m_1f_{27} + m_1f_{25} + m_1f_{29} - m_1f_{31})\sinh(m_1) + (f_{35} - 2f_{37} + 3f_{39} - 4f_{41} - n_2f_{36} + n_2f_{34} + n_2f_{38} - n_2f_{40} + n_2f_{42}) \times \cosh(n_2) + (-f_{36} + 2f_{38} - 3f_{40} + 4f_{42} - n_2f_{33} + n_2f_{35} - n_2f_{37} + n_2f_{39} - n_2f_{41})\sinh(n_2),$$

$$z_{41} = \frac{1}{m_1^2}\left(\left(\frac{1}{m^2h^2r}(2f_{22} + 2m_1f_{26} + 2f_{27} + n_2^2f_{33} + 2n_2f_{36} + 2f_{37})\right) - 2p_{46} - 2m_1p_{50} - 2p_{51} - n_1^2p_{57} - 2n_1p_{60} - 2p_{61}\right),$$

$$z_{42} = \frac{1}{m_1^2}\left(\frac{1}{rm^2h^3}\left(m_1^2(f_{25} + n_2f_{34} + f_{35}) - 6f_{23} - 3m_1^2f_{25} - 6m_1f_{28} - 6f_{29} - n_2^3f_{34} - 3n_2^2f_{35} - 6n_2f_{38} - 6f_{39} + d_4(d_{10} + m_1d_{12} + n_1l_7) - d_3(d_9 + d_{11} + l_8) + A(c_{11} + p_{13} + p_{15})\right) - m_1^2(p_{49} + n_1p_{58} + p_{59}) - d_2(d_6 + m_1d_8 + n_1l_5) + d_1(d_5 + d_7 + l_6) - Gr(c_9 + p_1 + p_3) - 6p_{47} - 3m_1^2p_{49} - 6m_1p_{52} - 6p_{53} - n_1^3p_{57}\right) + 3n_1^2p_{59} + 6n_1p_{62} + 6p_{63},$$

$$z_{43} = \frac{1}{mhr} - \frac{1}{m^2h^2r},\quad z_{44} = \frac{f_{33}}{mhr} - p_{57} - z_{41},$$

$$z_{45} = \frac{1}{m_1mhr} - \frac{1}{m_1m^2h^3r},$$

$$z_{46} = \frac{1}{m_1}\left(\frac{f_{25} + n_2f_{34} + f_{35}}{mhr} - z_{42} - p_{49} - n_1p_{58} - p_{59}\right),$$

$$z_{47} = \frac{1}{m^2h^3r} + z_{45}\sinh(m_1),$$

$$z_{48} = z_{43} + \frac{\cosh(m_1)}{m^2h^2r},\quad z_{49} = \frac{\sinh(m_1)}{mhr},$$

$$z_{50} = z_{44} + z_{42} + z_{41}\cosh(m_1) + z_{46}\sinh(m_1) + z_{37},$$

$$z_{51} = \frac{1}{m^2h^3r} + z_{45}m_1\cosh(m_1),\quad z_{52} = \frac{m_1\sinh(m_1)}{m^2h^2r},$$

$$z_{53} = \frac{m_1\cosh(m_1)}{mhr},$$

$$z_{54} = z_{42} + z_{46}m_1\cosh(m_1) + z_{41}m_1\sinh(m_1) + z_{38},$$

$$z_{55} = z_{47} + \frac{1}{mhr},\quad z_{56} = z_{48} - \frac{\cosh(m_1)}{mhr},$$

$$z_{57} = z_{49} + \frac{\sinh(m_1)}{mhr},\quad z_{58} = z_{50} - \frac{z_{39}}{mhr},$$

$$z_{59} = z_{52} + z_{51}m_1\sinh(m_1),\quad z_{60} = z_{53} - z_{51}m_1\cosh(m_1),$$

$$z_{61} = z_{54} - z_{40}z_{51},\quad z_{62} = z_{56} + z_{54}m_1\sinh(m_1),$$

$$z_{63} = z_{57} - z_{55}m_1\cosh(m_1),\quad z_{64} = z_{58} - z_{40}z_{55},$$

$$d_{20} = i\left(\frac{z_{59}z_{64} - z_{62}z_{61}}{z_{60}z_{64} - z_{59}z_3}\right),\quad d_{19} = \frac{-iz_{61} - z_{60}d_{20}}{z_{59}},$$

$$d_{18} = m_1d_{19}\sinh(m_1) - m_1d_{20}\cosh(m_1) - iz_{40},$$

$$d_{17} = d_{18} - d_{19}\cosh(m_1) + d_{20}\sinh(m_1) - iz_{39},$$

$$d_{16} = \frac{d_{20}}{mhr} + z_{45}d_{18} + iz_{46},\quad d_{15} = \frac{d_{19}}{m^2h^2r} + iz_{41},$$

$$d_{14} = \frac{d_{18}}{m^2h^3r} + iz_{42},\quad d_{13} = \frac{d_{17}}{mhr} + z_{43}d_{19} + iz_{44}.$$

References

Burns, J.C., Parks, T., 1967. Peristaltic motion. J. Fluid Mech. 29, 731–743.

Goldstein, J.L., Sparrow, E.M., 1977. Heat/mass transfer characteristic for flow in a corrugated wall channel. Trans. ASME J. Heat Transfer 99, 187–195.

Jang, J.Y., Chen, J.L., 1992. Forced convection in a parallel plate channel partially filled with a high porosity medium. Int. Commun. Heat Mass Transfer 19, 263–273.

Jang, J.H., Yan, W.M., 2004. Mixed convection heat and mass transfer along a vertical wavy surface. Int. J. Heat Mass Transfer 47, 419–428.

Kim, S.J., Choi, C.Y., 1996. Convective heat transfer in porous and overlying fluid layers heated from below. Int. J. Heat Mass Transfer 39, 319–329.

Kuznetsov, A.V., 1999. Fluid mechanics and heat transfer in the interface region between a porous medium and a fluid layer: a Boundary layer solution. J. Porous Media 2, 309–321.

Loharsabi, J., Sahai, V., 1998. Magneto hydrodynamic heat transfer in two phase flow between parallel plates. Appl. Sci. Res. 45, 53–66.

Malashetty, M.S., Leela, V., 1992. Magnetohydrodynamic heat transfer in two phase flow. Int. J. Eng. Sci. 30, 371–377.

Malashetty, M.S., Umavathi, J.C., Leela, V., 2001a. Magnetoconvective flow and heat transfer between vertical wavy wall and a parallel flat wall. Int. J. Appl. Mech. Eng. 6, 437–456.

Malashetty, M.S., Umavathi, J.C., Prathap Kumar, J., 2001b. Convective flow and heat transfer in an inclined composite porous medium. J. Porous Media 15, 15–22.

Malashetty, M.S., Umavathi, J.C., Prathap Kumar, J., 2004. Two fluid flow and heat transfer in an inclined composite porous and fluid layer. Heat Mass Transfer 40, 871–876.

Meyer, H.I., Garder, A.O., 1954. Mechanics of two immiscible fluids in porous media. J. Appl. Phys. 25, 1400–1406.

O'Brien, J.E., Sparrow, E.M., 1982. Corrugated-duct heat transfer, pressure drop, and flow visualization. Trans. ASME J. Heat Transfer 104, 410–416.

Ochoa-Tapia, J.A., Whitaker, S., 1998b. Momentum jump condition at the boundary between a porous medium and a homogeneous fluid: inertial effects. J. Porous Media 1, 201–217.

Ochoa-Tapia, J.A., Whitaker, S., 1998a. Heat transfer at the boundary between a porous medium and a homogeneous fluid: the one-equation model. J. Porous Media 1, 31–46.

Ostrach, S., 1952. An analysis of laminar free-convection flow and heat transfer about a flat plate parallel to the direction of the generating body force. NACA, TN-2635, Accession Number-93R12788, Documentation ID-19930083498.

Prathap Kumar, J., Umavathi, J.C., Biradar, Basavaraj M., 2011a. Mixed convection of magneto hydrodynamic and viscous fluid in a vertical channel. Int. J. Non-Linear Mech. 46, 278–285.

Prathap Kumar, J., Umavathi, J.C., Biradar, Basavaraj M., 2011b. Mixed convective flow of immiscible fluids in a vertical channel. Heat Transfer Asian Res. 40, 1–25.

Sahraoui, M., Kaviany, M., 1992. Slip and no-slip velocity boundary conditions at the interface of porous, plain media. Int. J. Heat Mass Transfer 35, 927–943.

Sahraoui, M., Kaviany, M., 1994. Slip and no-slip temperature boundary conditions at the interface of porous, plain media: convection. Int. J. Heat Mass Transfer 37, 1029–1044.

Saniei, N., Dini, S., 1993. Heat transfer characteristics in a wavy-walled channel. Trans. ASME J. Heat Transfer 115, 788–791.

Kuhn, Simon, Rudolf von Rohr, Philipp, 2008. Experimental investigation of mixed convective flow over a wavy wall. Int. J. Heat Fluid Flow 29, 94–106.

Umavathi, J.C., Ali, J. Chamkha, Abdul Mateen, Al-Mudhaf A., 2005. Unsteady two fluid flow and heat transfer in a horizontal channel. Heat Mass Transfer 42, 81–90.

Umavathi, J.C., Chamkha, A.J., Abdul Mateen, Prathap Kumar, J., 2008a. Unsteady magneto hydrodynamic two fluid flow and heat transfer in a horizontal channel. Int. J. Heat Technol. 26, 121–133.

Umavathi, J.C., Liu, I.C., Shaik Meera, D., 2008b. Unsteady flow and heat transfer of three immiscible fluids. Int. J. Appl. Mech. Eng. 13, 1079–1100.

Umavathi, J.C., Manjula, M.H., Pop, I., Liu, I.C., 2007. Flow and heat transfer of couple stress viscous fluids in a vertical channel. Int. J. Appl. Mech. Eng. 12, 537–555.

Umavathi, J.C., Shekar, M., 2011. Mixed convective flow of two immiscible viscous fluids in a vertical wavy channel with traveling thermal waves. Heat Transfer Asian Res. 40 (8), 721–743.

Umavathi, J.C., Liu, I.C., Shekar, M., 2012. Unsteady mixed convective heat transfer of two immiscible fluids confined between a long vertical wavy wall and a parallel flat wall. Appl. Math. Mech.-Engl. Ed. 33 (7), 931–950.

Vafai, K., Kim, S.J., 1990. Fluid mechanics of the interface region between a porous medium and a fluid layer: an exact solution. Int. J. Heat Fluid Flow 11, 254–256.

Vajravelu, K., 1989. Combined free and forced convection in hydromagnetic flows, in vertical wavy channels, with traveling thermal waves. Int. J. Engng. Sci. 27 (3), 289–300.

Vajravelu, K., Sastri, K.S., 1978. Free convective heat transfer in a viscous incompressible fluid confined between a long vertical wavy wall and a parallel flat wall. J. Fluid Mech. 86, 365–383.

Wang, C.C., Chen, C.K., 2001. Transient force and free convection along a vertical wavy surface in micropolar fluids. Int. J. Heat Mass Transfer 44, 3241–3251.

Wang, G., Vanka, S.P., 1995. Convective heat transfer in periodic wavy passages. Int. J. Heat Mass Transfer 38, 3219–3230.

Yao, L.S., 2006. Natural convection along a vertical complex wavy surface. Int. J. Heat Mass Transfer 49, 281–286.